Received: 30 May 2024 | Revised: 16 July 2024 | Accepted: 17 July 2024

DOI: 10.1111/mmi.15303

RESEARCH ARTICLE

WILEY

The dual role of a novel *Sinorhizobium meliloti* chemotaxis protein CheT in signal termination and adaptation

Alfred Agbekudzi[1] | **Timofey D. Arapov**[1] | **Ann M. Stock**[2] | **Birgit E. Scharf**[1]

[1]Department of Biological Sciences, Life Sciences I, Virginia Tech, Blacksburg, Virginia, USA

[2]Department of Biochemistry and Molecular Biology, Robert Wood Johnson Medical School, Rutgers University, Piscataway, New Jersey, USA

Correspondence
Birgit E. Scharf, Department of Biological Sciences, Life Sciences I, Virginia Tech, Blacksburg, VA 24061, USA.
Email: bscharf@vt.edu

Funding information
National Science Foundation, Grant/Award Number: MCB-1253234 and MCB-1817652

Abstract

Sinorhizobium meliloti senses nutrients and compounds exuded from alfalfa host roots and coordinates an excitation, termination, and adaptation pathway during chemotaxis. We investigated the role of the novel *S. meliloti* chemotaxis protein CheT. While CheT and the *Escherichia coli* phosphatase CheZ share little sequence homology, CheT is predicted to possess an α-helix with a DXXXQ phosphatase motif. Phosphorylation assays demonstrated that CheT dephosphorylates the phosphate-sink response regulator, CheY1~P by enhancing its decay two-fold but does not affect the motor response regulator CheY2~P. Isothermal Titration Calorimetry (ITC) experiments revealed that CheT binds to a phosphomimic of CheY1~P with a K_D of 2.9 μM, which is 25-fold stronger than its binding to CheY1. Dissimilar chemotaxis phenotypes of the Δ*cheT* mutant and *cheT* DXXXQ phosphatase mutants led to the hypothesis that CheT exerts additional function(s). A screen for potential binding partners of CheT revealed that it forms a complex with the methyltransferase CheR. ITC experiments confirmed CheT/CheR binding with a K_D of 19 μM, and a SEC-MALS analysis determined a 1:1 and 2:1 CheT/CheR complex formation. Although they did not affect each other's enzymatic activity, CheT binding to CheY1~P and CheR may serve as a link between signal termination and sensory adaptation.

KEYWORDS
carboxyl methylation, sensory adaptation, speed-variable flagellar motor, transmembrane receptors, two-component system

1 | INTRODUCTION

Motile bacteria have evolved diverse mechanisms for movement in the environment. They can swim to flee harm, reach an infection site, and facilitate host interactions (Erhardt, 2016). This motility behavior is carried out by efficient intracellular motors, which power intricately assembled structures like flagella and are controlled by a set of core and auxiliary chemosensory proteins. Flagellated bacteria are able to alternate between straight swimming paths or runs and random reorientations or tumbles to traverse a concentration gradient. This phenomenon known as a biased random walk (Berg, 1993) is mediated by a complex signal transduction system, which is best studied in the γ-proteobacterium *Escherichia coli* (for reviews, see Porter et al., 2011; Sourjik & Wingreen, 2012; Wadhams & Armitage, 2004).

Signaling in *E. coli* is initiated by a repertoire of chemoreceptors or Methyl Accepting Chemotaxis Proteins (MCPs), which are dimeric transmembrane proteins that form a stable, ternary complex with

two CheW adaptor protein monomers and a histidine kinase CheA dimer (Wadhams & Armitage, 2004). These complexes congregate into larger hexagonal arrays that allow for amplification of detected cues and cooperative signaling among different receptor types (Briegel et al., 2014; Parkinson et al., 2005; Yang & Briegel, 2020). Chemoreceptors regulate the autokinase activity of CheA, which autophosphorylates by catalyzing the hydrolysis of ATP to form CheA~P and then transfers its phosphoryl group to a conserved aspartate residue of the response regulator CheY (Levit et al., 1999). In *E. coli*, phosphorylated CheY (CheY~P) interacts with the flagellar motor protein FliM, altering flagellar rotation from the counterclockwise (CCW) default state of the flagellar motors, to the clockwise (CW) state resulting in a tumble reaction (Borkovich et al., 1989; Lukat et al., 1991; Welch et al., 1993). A phosphatase, CheZ, accelerates CheY~P dephosphorylation and therefore signal termination.

Through a mechanism known as adaptation, cells that navigate a stimulus gradient maintain their sensitivity to a broad range of concentrations by modulating kinase activity (for recent reviews, Tu, 2013; Vladimirov & Sourjik, 2009). The *E. coli* adaptation system is based on enzyme-catalyzed reversible additions of methyl groups to conserved glutamate residues in the cytoplasmic signaling domain of MCPs (Hazelbauer et al., 2008; Morgan et al., 1993; Weis & Koshland, 1988). Receptor methylation is generated by CheR, a constitutively active methyltransferase, while the CheA-dependent activated methylesterase CheB serves as an antagonist to CheR function (Borkovich et al., 1989; Hess et al., 1988; Vladimirov & Sourjik, 2009; Wadhams & Armitage, 2004; Yonekawa et al., 1983). The adaptation enzymes are tethered to the chemoreceptor cluster via a pentapeptide motif at the C termini of some MCPs (Barnakov et al., 1999; Lai et al., 2006; Wu et al., 1996). Upon binding of an attractant to an MCP, the rate of CheA autophosphorylation is reduced. As a result, the amount of CheB~P is reduced, causing an increase in the net level MCP methylation (Djordjevic & Stock, 1998; Kehry et al., 1983; Krembel et al., 2015). A second activity of CheB~P is the deamidation of conserved glutaminyl residues in the cytoplasmic domain of MCPs, converting them into new glutamate sites receptive to methylation by CheR (Kehry et al., 1983; Sherris & Parkinson, 1981).

E. coli and *Bacillus subtilis* share the basic, two-component system architecture but also exhibit notable differences. Unlike *E. coli*, attractant binding in *B. subtilis* activates the CheA kinase, increasing CheY~P levels. and thereby triggering CCW rotation of the motor and a run behavior (Garrity & Ordal, 1995, 1997). Thus, CCW rotation causes runs and CW rotation promotes cell tumbles in both organisms (Bourret et al., 1991; Stock et al., 1989). In addition to CheB and CheR being present in both organisms, *B. subtilis* expresses CheD, a deamidase, which positively regulates the autokinase activity of CheA when bound to the chemoreceptors (Kristich & Ordal, 2002; Rao et al., 2008). Furthermore, there are two phosphatases of CheY~P; CheC that is localized with the receptors, and FliY, an integral part of the *B. subtilis* flagellar motor C-ring (Bischoff & Ordal, 1992; Szurmant et al., 2004). A second function of CheD is regulated through CheC. The receptor-bound population of CheD is diminished through CheC-CheD interaction. This feed-forward regulatory mechanism downregulates CheA activity and the cellular levels of CheY~P. As CheY~P is being dephosphorylated by FliY and CheC, dissociated CheD binds to the chemoreceptors, thus restoring CheA autokinase activity (Rao et al., 2008; Rosario & Ordal, 1996). Analyses of *B. subtilis* and *E. coli* have revealed mechanistic differences in the way receptor methylation influences histidine kinase activity. *B. subtilis* maintains a steady level of methylated sites on MCPs, but changes in the methylation state of individual conserved glutamate residues dictate the activity of the kinase (Glekas et al., 2011; Rao et al., 2008; Walukiewicz et al., 2014). Thus, although CheB and CheR functions have been conserved in both species, their action promotes different outcomes.

Sinorhizobium meliloti controls its CW rotating peritrichous flagella to locate nutrients and germinating seeds and roots of its host *Medicago sativa* for the establishment of a nitrogen-fixing symbiotic relationship (Ashish, 2015; Götz & Schmitt, 1987). Sensing of host phytochemicals by *S. meliloti* MCPs direct movement of bacteria towards roots hairs, where the exchange of chemicals results in the invasion of the host root by the symbiont and ultimately in the formation of root nodules (Gage, 2004). *S. meliloti* has six transmembrane and two cytosolic chemoreceptors controlling its flagellar-driven movement (Meier et al., 2007). So far, the main ligands of McpT, McpU, McpV, McpX have been identified as broad-range of carboxylates, amino acids, short chain carboxylic acids, and quaternary ammonium compounds, respectively (Baaziz et al., 2021; Compton et al., 2018; Webb, Compton, et al., 2017; Webb, Karl Compton, et al., 2017).

S. meliloti and other related α-proteobacteria such as *Agrobacterium tumefaciens*, *Azospirillum brasilense*, and *Caulobacter crescentus* possess more than one response regulator species and have been known to lack a CheZ homolog (Miller et al., 2009; Scharf & Schmitt, 2002). Hence, signal termination is mediated by phosphoryl group transfer from the motor response regulator CheY2~P to CheA, which in turn transfers phosphoryl groups to a second response regulator, CheY1 (Attmannspacher et al., 2005; Riepl et al., 2008; Scharf & Schmitt, 2002; Sourjik & Schmitt, 1996). CheS, a small protein only present in a small group of related α-proteobacteria, promotes interaction between CheA and CheY1, which allows for the drainage of the phosphate sink (Dogra et al., 2012). Interaction of the phosphorylated motor response regulator (CheY2~P) with flagellar motors reduces flagellar rotary speed and mediates tumbles (Attmannspacher et al., 2005; Scharf & Schmitt, 2002; Schmitt, 2002; Sourjik & Schmitt, 1996).

S. meliloti possesses both adaptation proteins, and their target MCP glutamate residues are mostly conserved projecting similar adaptational mechanisms (Arapov et al., 2020; Meier et al., 2007). Our recent study of the adaptation system in *S. meliloti* revealed that CheR and CheB bind to the C-terminal chemoreceptor pentapeptide tether, a trait shared with the *E. coli* system (Agbekudzi & Scharf, n.d.). On the other hand, the presence of a deamidase CheD may suggest an adaptation system that is closer to that of *B. subtilis*. These similarities and variations profoundly justify further studies

of the *S. meliloti* adaptation module, and how it integrates into its chemotaxis system. In this work, the role of the *S. meliloti* chemotaxis protein CheT, which is encoded by the last gene in the chemotaxis operon (*che1*) downstream of *cheD*, was investigated (Sourjik et al., 1998). We present evidence that CheT is involved in the signal termination and adaptation pathway of *S. meliloti*.

2 | RESULTS

2.1 | Bioinformatics analyses predicts CheT to be a structural homolog of *E. coli* CheZ

The major chemotaxis operon *che1* in *S. meliloti* contains a gene of unknown function, which is the last gene in the operon downstream of *cheD*. The deduced primary sequence of the gene product is a protein with 124 amino acid residues (13.4 kDa), which we named CheT. It has no apparent homologs in paradigm models of bacterial chemotaxis, but *cheT* is similar to genes found in other, closely related alphaproteobacteria such as *Sinorhizobium medicae*, *Agrobacterium tumefaciens*, *Caulobacter crescentus*, *Rhizobium leguminosarum* and *Hoeflea* sp. 108 (Figure 1). Gene synteny of these orthologs is highly conserved, as they are the last gene in the major chemotaxis operons of each species, with the exception of *C. crescentus*, which has two additional chemotaxis genes in the operon 5′ of the *cheT* homolog. Their primary sequences exhibit varied identity of 81% (*S. medicae*), 70% (*A. tumefaciens*), 67% (*R. leguminosarum*), 28% (*Hoeflea* sp. *108*), and 20% (*C. crescentus*) (Figure 1). Across all genomes surveyed, the position of and distance between two residues, Asp-57 and Gln-61, are highly conserved. The DXXXQ sequence has been previously implicated as a phosphatase motif on the catalytic surface of CheZ (Liu et al., 2018; Zhao et al., 2002) suggesting that CheT is a CheZ-like phosphatase. AlphaFold (Varadi & Velankar, 2022) predicts the structure for a monomer of CheT to consist of two core alpha helices with two small C-terminal helices and largely unstructured N- and C-terminal regions (Figure 2a). Similarly, the crystal structure of the *E. coli* phosphatase CheZ exhibits two extended helices in each monomer of the dimeric protein. Interestingly, the conserved Asp and Gln in the phosphatase motif in both *E. coli* CheZ and *S. meliloti* CheT are similarly aligned on the helical coil. The position of their side chains in CheZ allows for efficient access to solvent and the CheY active site to catalyze the rapid dephosphorylation of CheY~P (Zhao et al., 2002). Therefore, we hypothesized that, despite sequence differences, CheT is a functional homolog of *E. coli* CheZ.

2.2 | CheT enhances dephosphorylation of CheY1~P but not CheY2~P

To experimentally corroborate the hypothesis from structure prediction that CheT is a CheZ phosphatase, we performed time-course phosphorylation assays using purified recombinant CheA, CheY2, and CheT in a molar ratio of 1:5:10. Following the autophosphorylation reaction of CheA with [γ-^{32}P]-ATP (Figure 3a lane 1), we initiated phosphotransfer by the addition of CheY2. Subsequently, equal volumes of buffer or CheT were

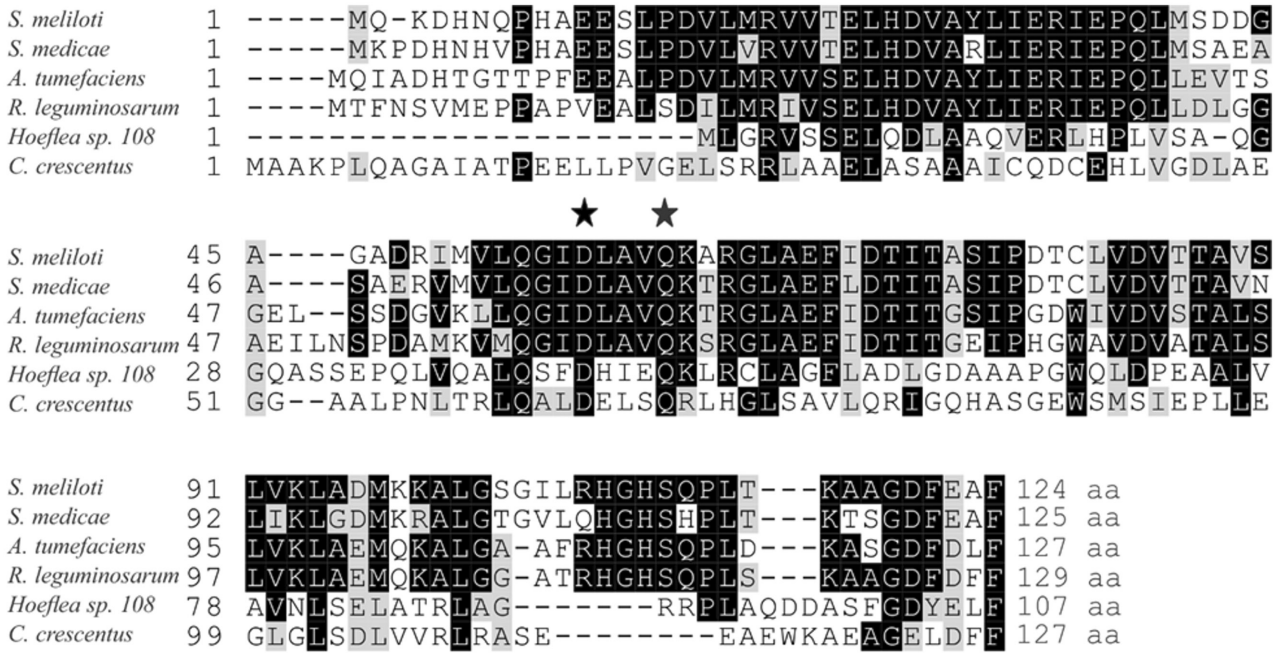

FIGURE 1 Alignment of the amino acid sequence of *S. meliloti* CheT (NP_384751.1) with five paralogues from related alphaproteobacteria. *Sinorhizobium medicae* (*YP_001325935.1*), *Agrobacterium tumefaciens* (WP_003493786.1), *Rhizobium leguminosarum* (WP_003588573.1), *Hoeflea* sp. 108 (WP_018430236.1), and *Caulobacter crescentus* CheU (NP_419258.1). GenBank accession numbers are given in parentheses. Sequences were aligned through ClustalOmega. Black shading indicates identical residues and gray shading indicates residues with similar side change properties. Stars indicate conserved residues indicative of a putative (DXXXQ) CheZ-like phosphatase motif.

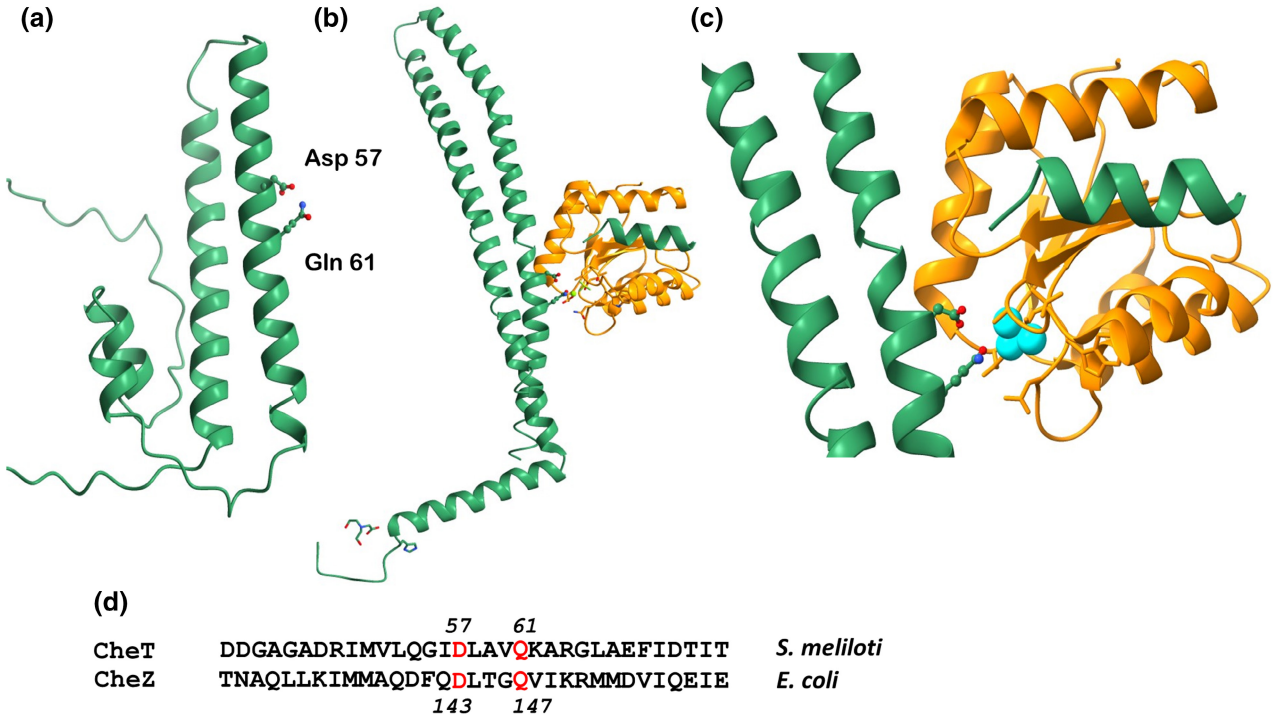

FIGURE 2 Structure prediction of *S. meliloti* CheT and comparison to *E. coli* CheZ. (a) Predicted AlphaFold structure of a monomer of *S. meliloti* CheT. The side chains of the conserved Asp and Gln residues of the putative DXXXQ phosphatase motif are shown as ball and sticks with red and blue representing oxygen and nitrogen atoms, respectively. (b) Crystal structure of *E. coli* CheZ bound to CheY (PDB# 1KMI). (c) An enlarged ribbon image of B the active site of CheY (orange), BeF_3^- (cyan), and CheZ (green) with Asp and Gln residues of the DXXXQ phosphatase motif shown as ball and sticks with oxygen (red) and nitrogen atoms (blue). (d) A sequence segment of amino acid residues bearing the DXXXQ phosphatase motif in *S. meliloti* CheT and *E. coli* CheZ.

simultaneously added to the reaction mixtures to determine the effect of CheT on CheY2~P. The reactions, with or without CheT, were terminated after 20, 40, 60, and 80 seconds (Figure 3a lanes 2–9), separated by SDS-PAGE and exposed to a phosphoscreen. Autodephosphorylation of CheY2~P occurred over time; however, no differences in the CheY2~P band intensity were observed in the absence or presence of CheT (Figure 3a). This result allows the conclusion that CheT does not enhance the dephosphorylation of CheY2~P.

Next, we performed a similar time course experiment to analyze the effect of CheT on CheY1~P following phosphotransfer from CheA (Figure 3b) and a CheA/CheS (CheA/S) complex (Figure 3c). In both experiments, after CheA autophosphorylation with [γ-^{32}P]-ATP (Figure 3b,c, lane 1), we observed phosphotransfer to CheY1 (Figure 3b,c, lane 2). The addition of CheT (Figure 3b,c, lane 3) resulted in the complete disappearance of the CheY1~P band after 10 s. This experiment identified CheT as CheY1-specific phosphatase.

2.3 | Kinetics of CheY1~P dephosphorylation by CheT

To determine the kinetics of CheY1~P dephosphorylation by CheT and identify the role of the phosphatase motif residues Asp-57 and Gln-61, we performed the assay with purified CheA~^{32}P (Figure 4a–c) and CheA~^{32}P/CheS (Figure 4d–f). The yield of phosphorylated CheA was approximately 5%, different from our previous study with 47% (Dogra et al., 2012). Therefore, reactions were carried out at molar CheA, CheY1, and CheT ratios of 0.5:1:0.1. Phosphotransfer reactions from purified CheA~^{32}P were initiated by the addition of CheY1. Subsequently, CheT, CheT-D57A, or CheT-Q61A were added to the individual phosphorylation reactions and terminated at times indicated. Samples were separated by SDS-PAGE, and the gel was exposed to a phosphor-storage screen. The exposed screen was scanned, a digital image obtained using an Amersham Typhoon scanner, and band intensities analyzed with ImageQuant™ TL 10.1 software. CheY1~P bands were significantly reduced in the presence of CheT, however, the addition of CheT variants had no effect on CheY1~P band intensities (Figure 4a,b). The deduced decay curve (Figure 4c) revealed that CheT accelerated CheY1~P dephosphorylation by two-fold, reducing its half-life from 26 to 13 s. In contrast, the half-life of CheY1~P in the presence of the phosphatase motifs variants CheT-D57A and CheT-Q61A (30 and 22 s) were similar to that in the absence of CheT. These results indicate a role for Asp-57 and Gln-61 in the catalysis of CheY1 dephosphorylation by CheT. Similarly, analyses of the band intensities of CheY1~P following phosphorylation by CheA~^{32}P/CheS (Figure 4d,e) demonstrated that CheT enhances CheY1~P dephosphorylation two-fold by reducing its half-life from 34 to 17 s (Figure 4f). Again, the putative phosphatase motif CheT variants had no effect on the half-life of

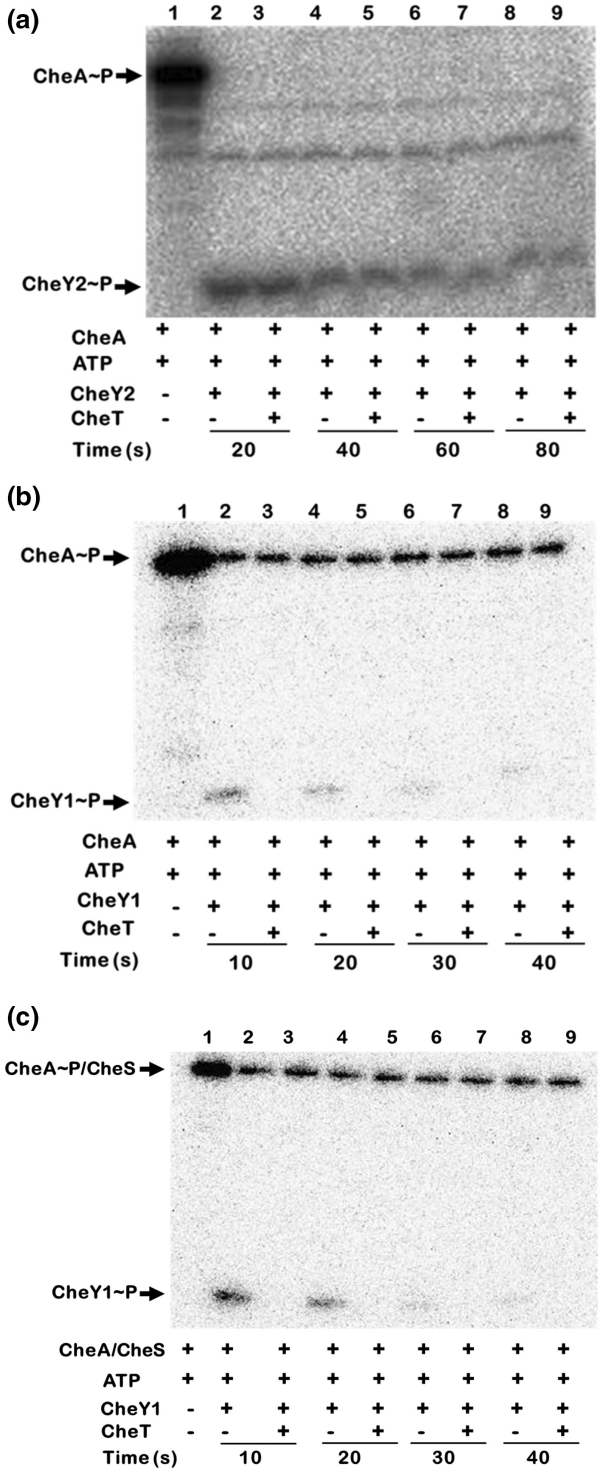

FIGURE 3 Dephosphorylation of CheY1 and CheY2 in the presence of CheT. Reactions contained 5 μM CheA, 5 μM CheA/CheS, 25 μM CheY2 or CheY1, 50 μM CheT and 0.6 mM 10 μCi [γ-^{32}P]-ATP in $TEDG_{10}$ buffer and were performed at room temperature. (a) Time course of CheY2~P dephosphorylation after phosphotransfer from CheA~P. (b) Time course of CheY1~P dephosphorylation after phosphotransfer from CheA~P. (c) Time course of CheY1~P dephosphorylation after phosphotransfer from CheA~P/CheS. Samples were separated using a 15% SDS-PAGE followed by overnight exposure of a storage phosphoscreen. A digital image was produced from laser-induced excitation of the phosphoscreen with the Amersham Typhoon FLA 950 imager. The lower molecular weight band with constant intensity seen in (a) likely represents a phosphorylated CheA degradation product.

CheY1~P (Figure 4f). These results suggest that CheT dephosphorylation of CheY1~P is not influenced by upstream phosphorylation events. These results provide a role of CheT and its phosphatase motif in the dephosphorylation of CheY1~P. They also suggest that CheS has no effect on this catalytic interaction. It is worth noting that the observed effect of CheT on the half-life of CheY1~P was performed at a molar excess of CheY1 over CheT (Figure 4), while the experiment showing that CheT is ineffective on CheY2~P was performed at a molar excess of CheT over CheY2~P (Figure 3). This result further strengthens the conclusion that the phosphatase activity CheT is specific for CheY1~P.

2.4 | CheT binds strongly to CheY1~P

The enzymatic activity of CheT on CheY1 implies that both proteins closely interact with each other. To investigate their interaction, we employed Isothermal Titration Calorimetry (ITC) to determine the affinity of CheT to CheY1 and a phosphomimic complex of CheY1 (CheY1-BeF_3). We observed exothermic heat changes for both protein pairs, producing dissociation constants (K_D) of 75 and 2.9 μM, respectively (Figure 5a,b). To test the contribution of the phosphatase DXXXQ motif in binding, we titrated CheT-D57A with CheY1 and CheY1-BeF_3^-. The exothermic heats from the binding interactions resulted in K_Ds of 48 μM and 11 μM, respectively, inferring that the mutation in the phosphatase motif affects binding to CheY1 and its phosphomimic form by increasing the affinity of CheT-D57A for CheY1 by 1.5-fold while decreasing the affinity of CheT-D57A for CheY1-BeF_3^- by four-fold. (Figure 5c,d).

2.5 | Phenotypic analysis of an *S. meliloti* strain lacking *cheT*

To gauge the function of CheT in chemotaxis, an in-frame deletion was introduced into the *S. meliloti* wild-type strain (RU11/001), and the chemotactic ability of the resulting mutant strain (RU11/319) was assessed and compared to six other chemotaxis deletion mutants (Figure S1). The Δ*cheT* mutant strain exhibited a 50% reduction in swim ring diameter on Bromfield soft agar plates compared to the wild type. This chemotaxis defect could be fully restored by complementation with a *cheT*-expressing plasmid. Deletions of *cheA*, *cheD*, *cheR*, or *cheY2* were more detrimental than that of *cheT*, while the deletion of *cheY1* was less severe. The *cheB* deletion strain displayed the most similar reduction in swim ring size to the Δ*cheT strain*.

To further assess how chemotaxis is affected by the deletion of *cheT*, we used computerized motion analysis to quantify the average free-swimming velocity of a population of cells. The swimming speed of *S. meliloti* is controlled by the levels of phosphorylated CheY2

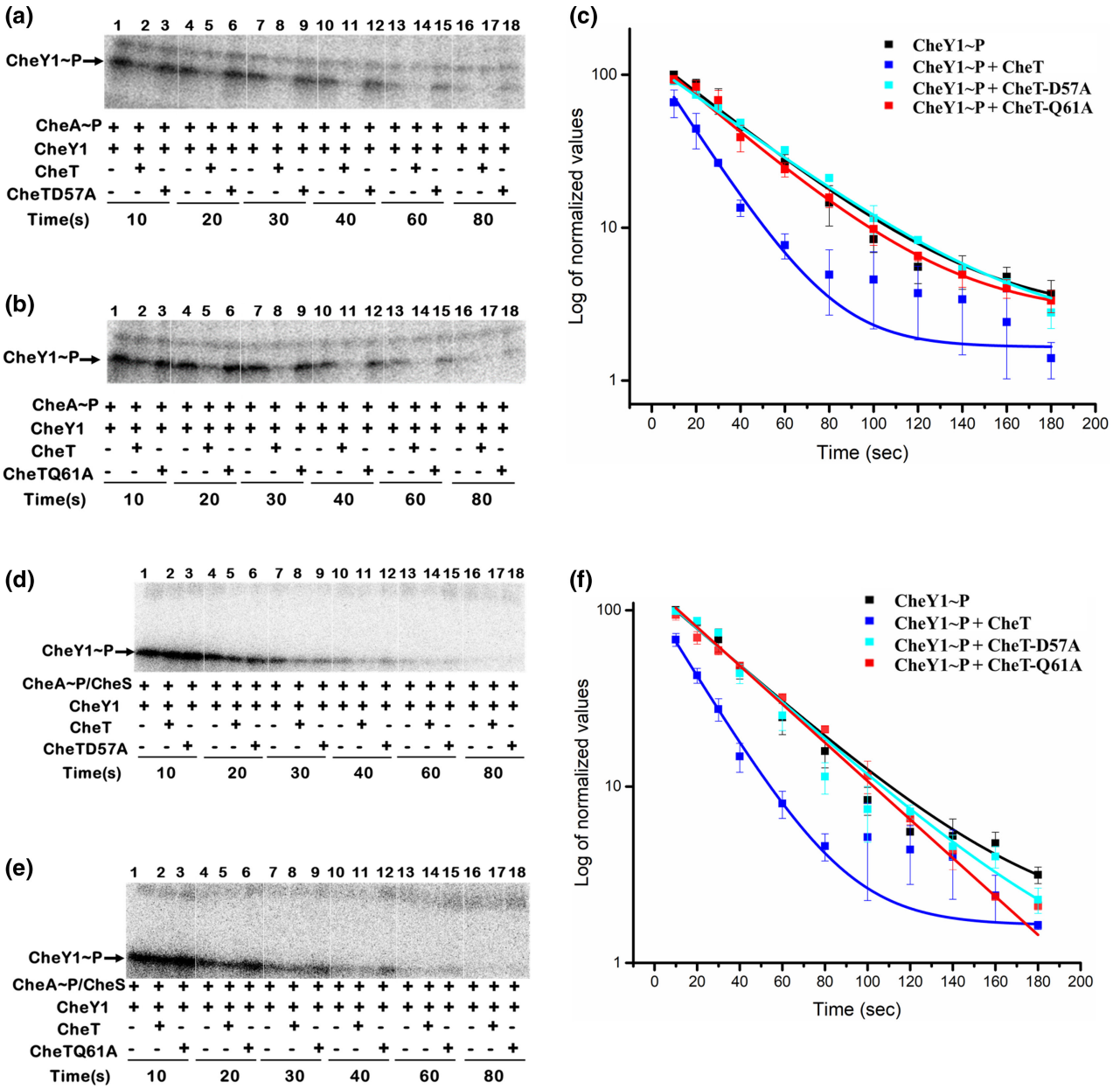

FIGURE 4 Kinetics of CheY1~P dephosphorylation in the presence of CheT and its variants. Reactions were carried out at molar CheA~P or CheA~P/CheS, CheY1, and CheT ratios of 0.5:1:0.1. (a) Digital image of CheY1~P dephosphorylation after phosphotransfer from CheA~P in the presence of CheT and CheT-D57A. (b) Digital image of CheY1~P dephosphorylation after phosphotransfer from CheA~P in the presence of CheT and CheT-Q61A. (c) A decay curve of CheY1~P dephosphorylation normalized to CheY1~P at 10 s. (d) Digital image of CheY1~P dephosphorylation after phosphotransfer from CheA~P/CheS in the presence of CheT and CheT-D57A. (e) Digital image of CheY1~P dephosphorylation after phosphotransfer from CheA~P/CheS in the presence of CheT and CheT-Q61A. (f) A decay curve of CheY1~P dephosphorylation normalized to CheY1~P at 10 s. Data points are the means from three replicates of CheY1~P pixel intensity and error bars reflect standard deviation determined with Amersham Typhoon image analyzer software. The exponential decay function was used to fit the curves.

(Sourjik & Schmitt, 1996). A low swimming speed is indicative of high levels of CheY2~P, whereas a high swimming speed is the result of low levels of CheY2~P. Attractant stimulation inhibits CheA activation and subsequently reduces phosphorylation of CheY2 causing a 10% increase in swimming speed in wild type (Figure 6a) (Meier et al., 2007). Consequently, deletion of *cheA* or *cheY2* resulted in an increased swimming speed that is not elevated when cells were stimulated with proline (Figure 6a) (Meier et al., 2007; Sourjik & Schmitt, 1996). On the other hand, the swimming speeds of non-stimulated *cheB*, *cheY1*, and *cheS* deletion strains were decreased, because CheB and CheY1 compete with CheY2 in phosphoryl groups from CheA, and CheS enhances phosphotransfer to CheY1 (Sourjik & Schmitt, 1996) (Figure 6a). Upon attractant stimulation, swimming speeds of these strains increased due to decreasing CheY2~P levels. Strains lacking *cheD* or *cheR* exhibited a fast-swimming phenotype in the absence and presence of the attractant. This phenotype is shared with the *cheT* deletion strain suggestive

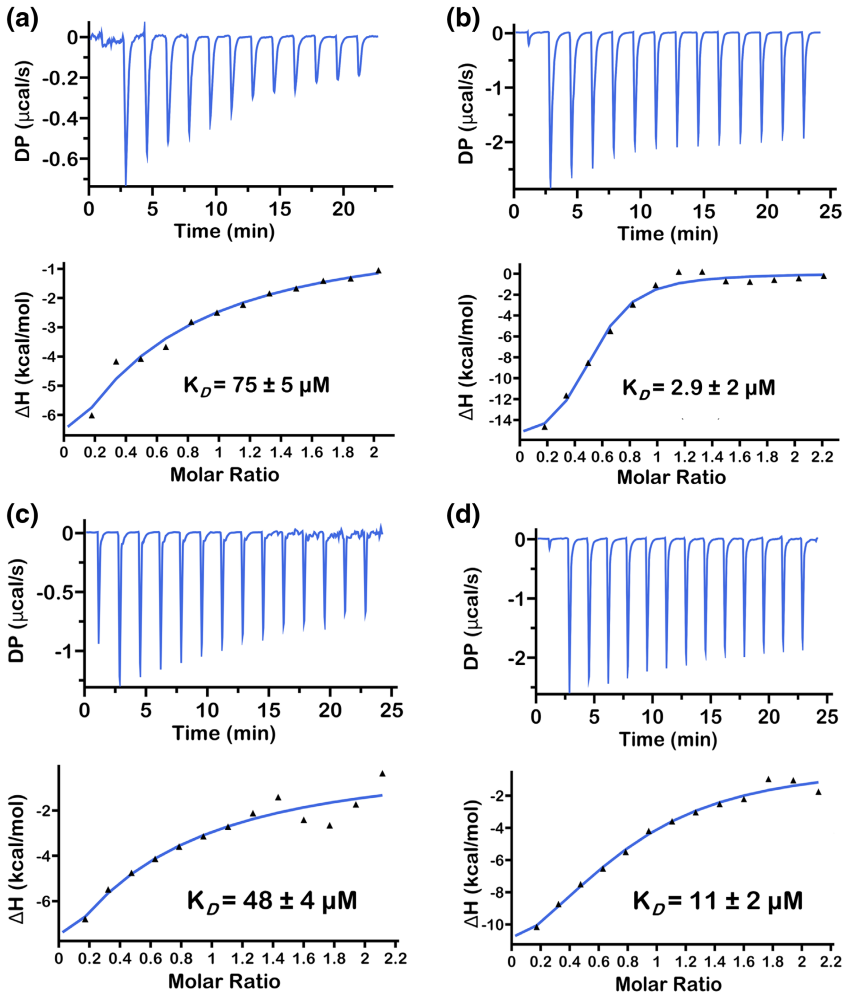

FIGURE 5 Isothermal titration calorimetry depicting the binding interaction. (a) CheT and CheY1, (b) CheT and CheY1-BeF_3^-, (c) CheTD57A and CheY1, (d) CheTD57A and CheY1-BeF_3^-. Upper panels: Raw data for the titration of 535 µM CheT with 50 µM CheY1 for Figure (a, b) and 300 µM CheTD57A with 300 µM CheY1 for Figure (c, d). Lower panels show the means and standard deviations of the dissociation constants, and the K_Ds generated from the normalized and dilution-corrected integrated peak areas of the raw titration data from three replicates. Data were fitted using the "one set of sites model" of the Malvern MicroCal PEAQ-ITC Analysis Software.

of low CheY2~P levels (Figure 6a,b). Bioinformatics and enzymatic analyses identified two conserved residues in CheT that are critical for phosphatase activity in *E. coli* CheZ and its homologs (Figures 1 and 4) (Liu et al., 2018; Zhao et al., 2002). To test whether these residues are important for CheT function, we created two mutant strains with Asp-57 and Gln-61 replaced with alanine residues. When this strain was subjected to swimming speed analysis, we recorded increased swimming velocity similar to the *cheT* strain. However, different from the *cheT* deletion strain, when stimulated with an attractant, the swimming speed further increased (Figure 6b). In conclusion, deletion of *cheT* caused a chemotaxis defect in *S. meliloti* resulting in a fast-swimming phenotype and insensitivity to attractant stimulation, whereas mutations in the phosphatase motif also caused mutant cells to swim fast but they could be stimulated with an attractant. These differences in chemotactic behavior suggest that CheT has a function in addition to its phosphatase activity on CheY1~P.

2.6 | CheT forms a complex with CheR

Due to the differences in the *cheY1* deletion and phosphatase mutants, we hypothesized that CheT might have a dual role, which could explain the unexpected phenotype of the *cheT* mutants. To test the interaction of CheT with other *S. meliloti* chemotaxis proteins, we used an in-vitro chemical crosslinking assay. CheT and its putative target proteins were crosslinked with 1% glutaraldehyde and separated electrophoretically via SDS-PAGE. Subsequent detection was achieved using an anti-CheT antibody. From the banding pattern on the immunoblot we inferred that CheT migrates according to its predicted molecular weight at 13.4 kDa and has a strong tendency to dimerize despite the presence of a reducing agent (Figure 7a, lane 1). The crosslinking agent further promoted dimerization and completely depleted the monomer pool (Figure 7a, lane 2). Out of eight chemotaxis proteins tested, only the addition of CheR (34 kDa) to the crosslinking reaction resulted in a significant change in banding pattern. Two new major bands emerged, migrating at approximately 45 and 90 kDa, which concurred with a reduction in CheT-dimer band intensity (Figure 7a, lane 6). Both bands are indicative of the formation of a 1:1 and a 2:2 CheR/CheT complex, respectively. In conclusion, data obtained from these crosslinking experiments revealed a putative interaction between CheT and CheR. It should be noted that a weak crosslinked band emerged in the reaction with CheY1, which is in line with the ITC data (Figure 5a). To quantify the interaction of CheT and CheR, we subjected CheR to microcalorimetric titrations with CheT, which produced exothermic binding heats with a

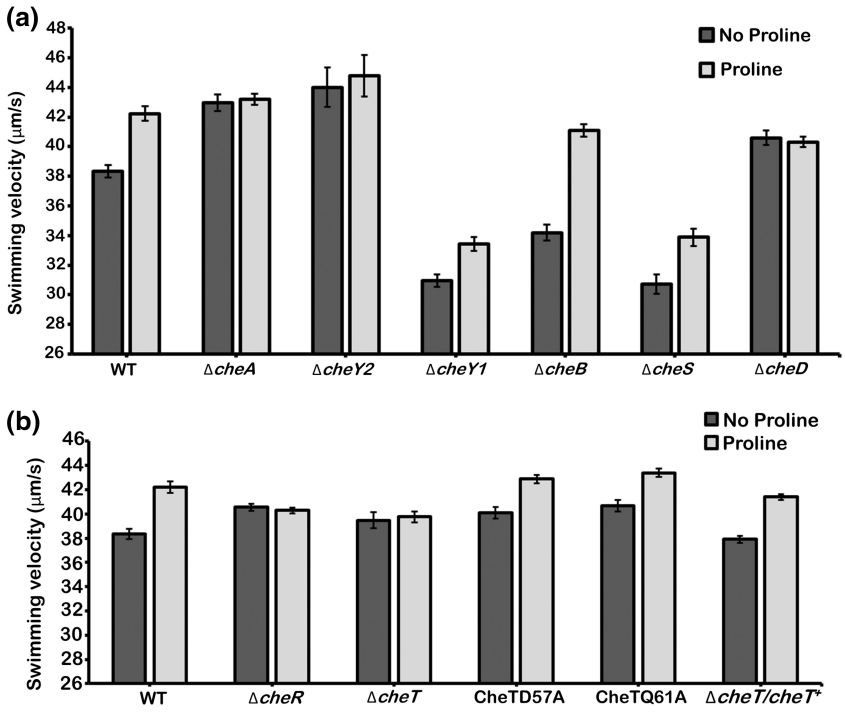

FIGURE 6 Free swimming speeds of *S. meliloti* strains before and after the addition of the attractant proline. Values are the means and standard deviations from at least three biological replicates. The dark and light gray bars represent swimming velocity of cells before and after stimulation with 10 mM proline, respectively. (a) WT (RU11/001), Δ*cheA* (RU11/310), Δ*cheY2* (RU11/307), Δ*cheY1* (RU11/308), Δ*cheB* (RU11/312), Δ*cheS* (RU11/408) and Δ*cheD* (RU11/411). (b) WT (RU11/001), Δ*cheR* (RU11/306), Δ*cheT*, (RU11/319); CheTD57A (BS190), CheTQ61A (BS170), and Δ*cheT*/*cheT*$^{+}$, Δ*cheT* (RU11/319) with pBBR1MCS-2-*cheT* (pBS445).

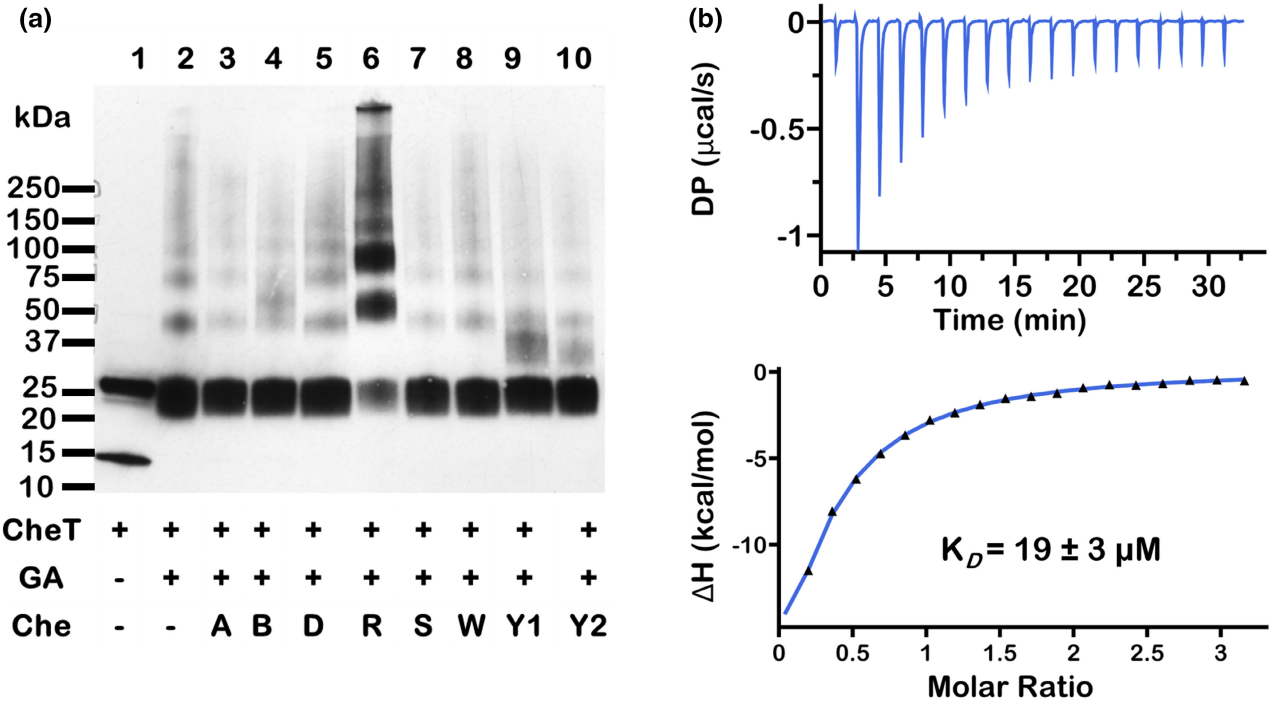

FIGURE 7 Biochemical analyses to assess the binding of *S. meliloti* CheT and CheR. (a) Crosslinking studies of CheT (0.7 μM) with CheA, CheB, CheD, CheR, CheS, CheW1, CheY1, and CheY2 (0.7 μM) using glutaraldehyde (GA) for 45 min at room temperature. Products were separated by gradient gel electrophoresis and probed with an anti-CheT antibody. (b) Isothermal titration calorimetry of recombinant CheR (30 μM) and CheT (500 μM). The upper panel shows the raw titration data while the lower panel depicts integrated raw data to obtain a K_D of 19 μM. K_D generated from the normalized and dilution corrected integrated peak areas of the raw titration data. The number and error are the mean and standard deviation of the K_D value from three experimental replicates. Data were fitted using the "one set of sites model" of the Malvern MicroCal PEAQ-ITC Analysis Software.

derived K_D of 19 μM (Figure 7b). In summary, CheT binds to both CheY1 and CheR with similar binding affinities.

2.7 | CheT exists as a homodimer and forms a heterooligomeric complex with CheR

E. coli CheZ is a homodimer with two core amphipathic helices from each monomer forming the interaction face (Blat & Eisenbach, 1996a, 1996b; Zhao et al., 2002). Therefore, we sought to investigate whether CheT has a similar oligomeric state. To determine the molecular weight of CheT in solution we employed Size-Exclusion Chromatography coupled with Multi-Angle Light Scattering (SEC-MALS), which allows the molecular size determination of purified proteins and protein complexes (Some et al., 2019). CheT has a molecular weight of 13.4 kDa and produced an elution peak with a calculated molecular weight of 26 kDa (Figure 8a). Thus, like CheZ, *S. meliloti* CheT forms a stable homodimer in solution. CheR produced a single peak suggestive of a monomer (Figure 8b). To establish the stoichiometry of the CheT and CheR complex, an equimolar mixture of the two proteins was subjected to SEC-MALS analysis. We observed the emergence of three elution peaks with Peak 1, 2, and 3 consistent with a 34-kDa CheR monomer, a 47-kDa CheR/CheT (1:1) complex, and a 60-kDa CheR/CheT (1:2) complex

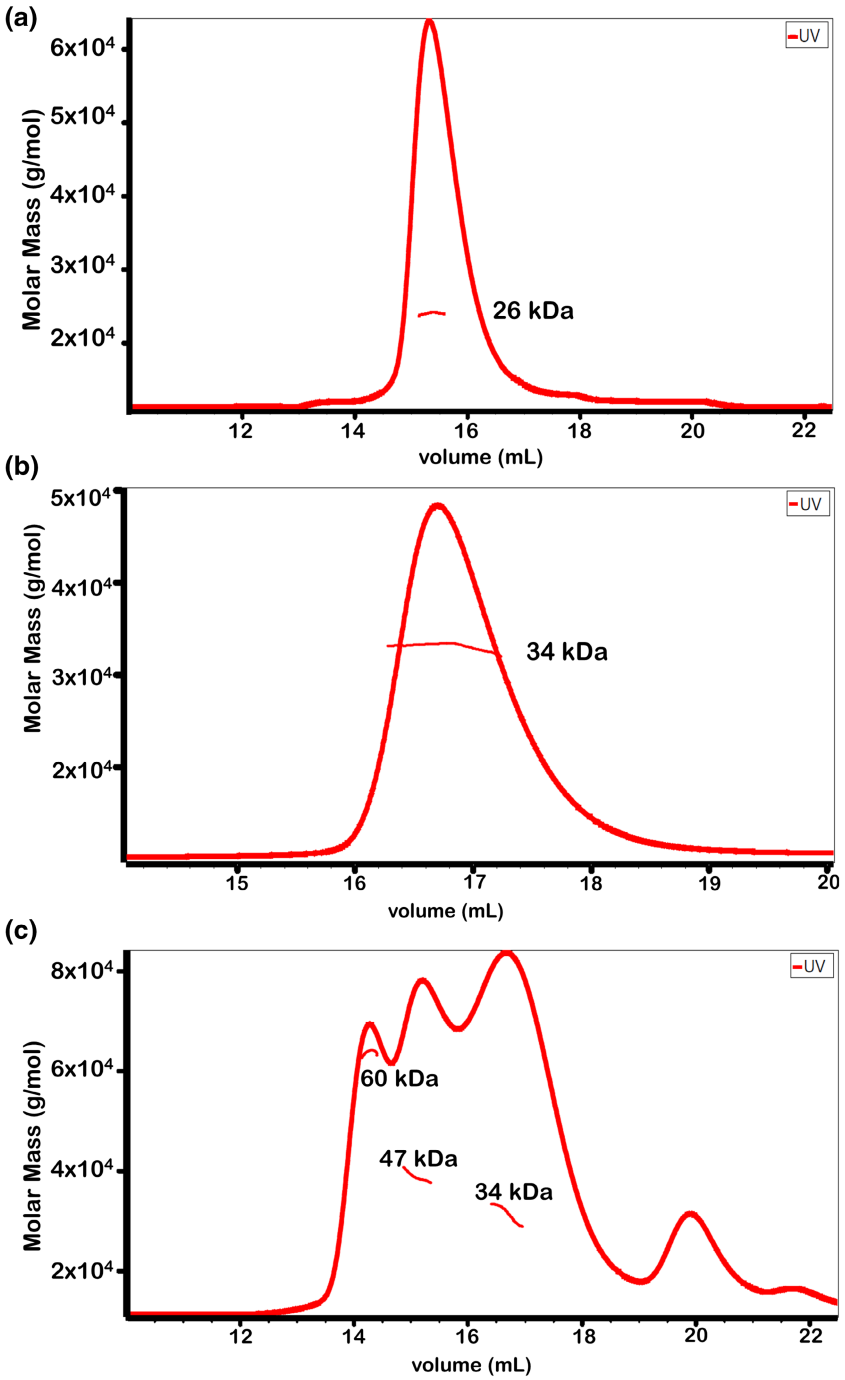

FIGURE 8 SEC-MALS analysis of CheT, CheR, and CheT/CheR mixture. Molar masses were calculated using measurements taken from the UV detector, laser monitor correction modes, and RI (refractive index) signals as a function of elution volume. The molar mass measurement of 10,000 g/mol represents 10 kDa. (a) CheT (13.4 kDa) elutes as dimer at approximately 26 kDa. (b) CheR (34 kDa) elutes as monomer. (c) Analysis of a CheR and CheT (1:1 molar ratio) mixture incubated for 30 min prior to loading on the column generated three significant peaks with calculated molecular masses consistent with CheR (34 kDa), and two complexes composed of a CheT monomer and a CheR monomer (47 kDa), and a CheT dimer and a CheR monomer (60 kDa), respectively.

(Figure 8c). These results confirm the complex formation between CheT and CheR.

2.8 | The complex formation between CheT and CheR does not affect CheT phosphatase activity

Next, we performed a phosphorylation assay to test if the CheT/CheR complex formation affects dephosphorylation of CheY1~P by CheT. Experiments were performed similarly to those shown in Figure 4, but in the presence of CheR. Phosphotransfer from CheA~P to CheY1 was initiated and CheY1~P band intensity measured over time following the addition of CheT and CheR in a 1:1 and 1:3 ratio (Figure 9). No difference in CheT-mediated CheY1~P dephosphorylation was observed in the presence of CheR. This suggests that the presence of CheR had no effect on CheT phosphatase activity under these experimental conditions.

2.9 | CheR methylation of McpX is unaltered by CheT

To test whether CheT affects methyltransferase activity of CheR, we applied a tritium-based in-vitro methylation assay as developed for *E. coli* chemoreceptors (Barnakov et al., 1998). We chose McpX, which detects quaternary ammonium compounds, as substrate for methylation. McpX was overexpressed in *E. coli* strain Lemo21 (DE3), and McpX-containing membrane vesicles were isolated. These were then incubated with CheR in the presence of [^{3}H]-S-adenosyl-L-methionine (SAM[^{3}H]) and aliquots withdrawn at different time points. Samples were separated via SDS-gel electrophoresis and the release of [^{3}H]-methanol from alkali-hydrolyzed gel fragments containing McpX was determined. Over a time-course of 15 min, McpX methylation increased linearly. Yet, the addition of CheT had no significant effect on CheR methylation activity (Figure 10) Next, we analyzed methylation of McpX in the presence of one of its ligands, choline (Shrestha et al., 2018; Webb, Karl Compton, et al., 2017). In analogy to *E. coli* MCPs, the addition of a ligand should increase receptor methylation in vitro (Spiro et al., 1997). Nonetheless, this was not the case for McpX (Figure 11). We also tested whether divalent cations, reducing (DTT) or chelating (EDTA) agents were required for CheT function. However, no significant change in McpX methylation was observed, with one exception; the addition of 5 mM $MgCl_2$ slightly reduced activity (Figure 11), although this effect was not consistently observed in all experimental variations. It has been reported that cyclic-di-GMP (c-di-GMP) is an activator for the CheR-binding protein MapZ in *Pseudomonas aeruginosa* (Orr & Lee, 2016; Yan et al., 2018). Therefore, we assayed McpX methylation by CheR in the presence of CheT and c-di-GMP but found no significant impact. Finally, the methyltransferase activity of copurified CheR/CheT was compared to that of CheR, again without observing any difference in McpX methylation. To assay a different CheR substrate, we purified membrane vesicles containing McpU. Yet, we were unsuccessful in determining conditions at which McpU was methylated by CheR. In conclusion, CheT had no effect on McpX methylation by CheR under these assay conditions.

3 | DISCUSSION

Previous investigations of the *S. meliloti* chemotaxis signaling pathway had focused on chemoreceptor function, intracellular phosphotransfer reactions, and composition of the chemotactic signaling

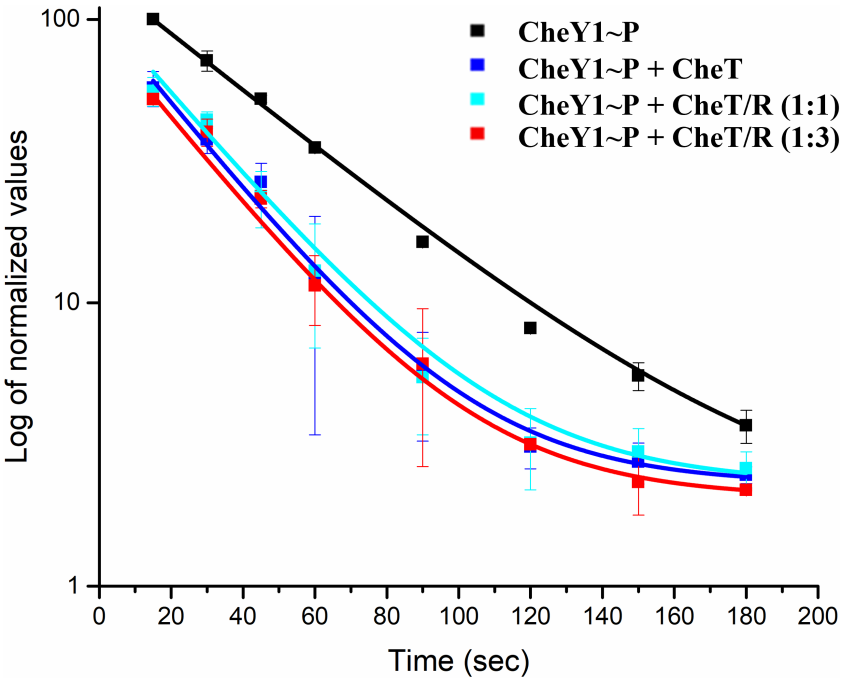

FIGURE 9 Kinetics of CheY1~P dephosphorylation in the presence of CheT and CheR in molar ratios of 1:1 and 1:3. Data points are the means from three replicates measurements of CheY1~P pixel intensity and error bars reflect standard deviation determined with using Amersham Typhoon image analyzer software. The exponential decay function was used to fit the curve.

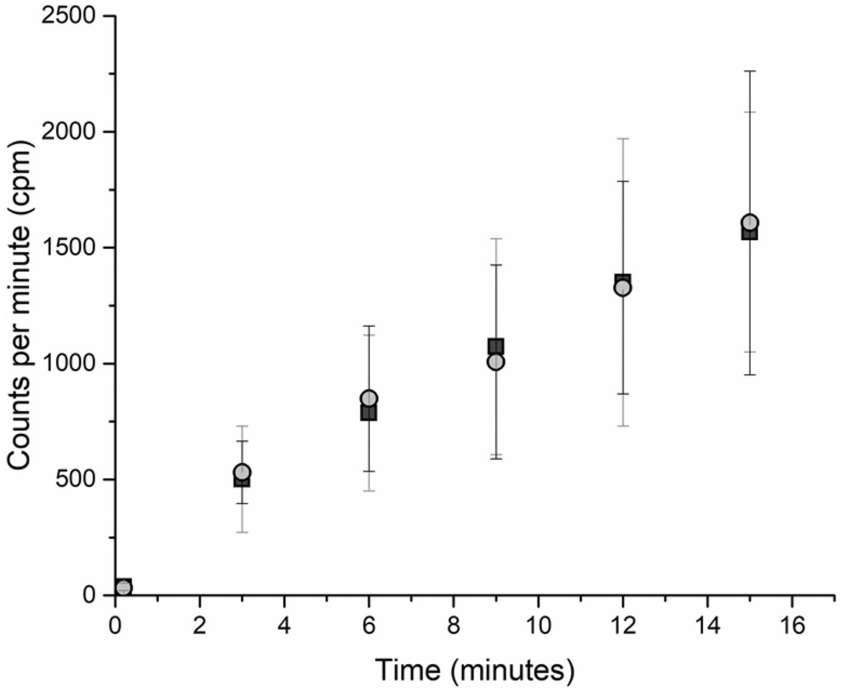

FIGURE 10 Time course of McpX methylation by CheR using [^{3}H]-S-adenosylmethionine (SAM[^{3}H]) as substrate. Reactions of 1.2 μM McpX in membrane vesicles with 0.2 μM CheR and 50 μM SAM were incubated for 0.2, 3, 6, 9, 12, and 15 min at room temperature, and stopped by incubation at 100°C in the presence of Laemmli buffer. Black squares and gray circles represent signals represent the mean derived from three replicates in the absence and presence of 4.6 μM CheT, respectively, error bars derived from the standard deviation of three replicates.

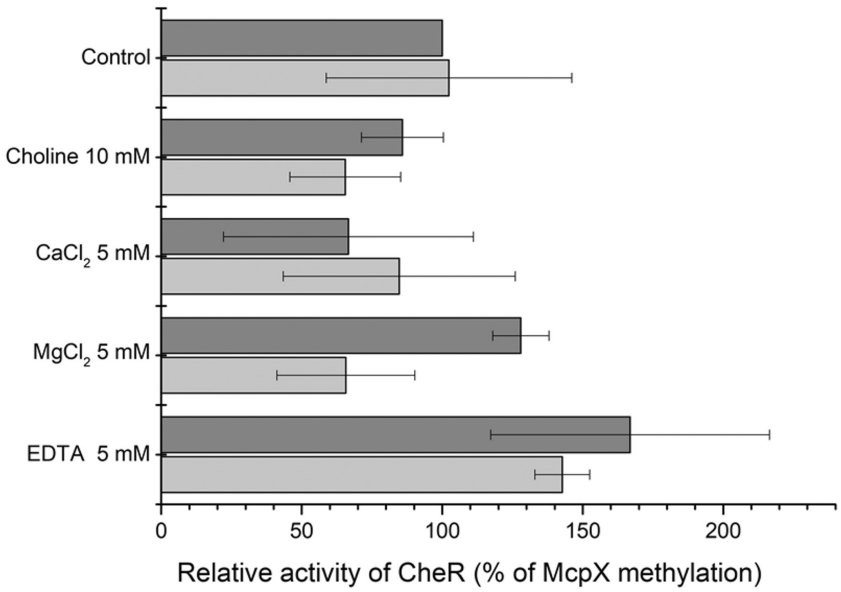

FIGURE 11 McpX methylation by CheR using [^{3}H]-S-adenosylmethionine (SAM[^{3}H]) as substrate with various supplements and a TGD buffer control. Reactions of 1.2 μM McpX in membrane vesicles with 0.2 μM CheR and 50 μM SAM[^{3}H] were incubated for 15 min at room temperature and stopped by incubation at 100°C in the presence of Laemmli buffer. All reactions were performed in TGD buffer with the specified additive for each condition. Dark and light gray bars represent the mean derived from three replicates in the absence and presence of 4.6 μM CheT.

complex (Compton et al., 2018; Dogra et al., 2012; Riepl et al., 2008; Scharf & Schmitt, 2002; Sourjik & Schmitt, 1996; Webb et al., 2014; Webb, Karl Compton, et al., 2017). This present work uncovered the role of CheT, encoded by the last gene in the chemotaxis operon, as a phosphatase specific for the phosphate sink response regulator, CheY1. Further studies revealed an additional role of CheT in adaptation that is not yet fully understood but sets apart the *S. meliloti* chemotaxis system even further from the enteric model.

Some information can be deduced through a comparison of chemotactic adaptation enzymes across species. The canonical adaptation system in *E. coli* employs CheR and CheB to modify conserved glutamate residues in the signaling domains of MCPs (Simms et al., 1987). Both proteins bind to high-abundance MCPs in *E. coli* via a C-terminal pentapeptide motif that serves as a tether in the chemoreceptor array (Lai et al., 2006; Wu et al., 1996). In *S. meliloti*, four of the eight chemoreceptors (including McpX) possess a conserved pentapeptide motif (Meier et al., 2007). However, these MCPs are not present at high abundance, but only represent 13% of the total receptor pool, compared to 93% in *E. coli* (Agbekudzi & Scharf, n.d.; Meier et al., 2007; Zatakia et al., 2018). Furthermore, *S. meliloti* CheR varies from *E. coli* CheR in lacking all residues in the beta-subdomain required for pentapeptide binding, a characteristic shared with closely related alphaproteobacteria (Perez & Stock, 2007). Regardless, we discovered that *S. meliloti* CheR and

activated CheB bind to pentapeptide-bearing chemoreceptors (Agbekudzi & Scharf, n.d.). In addition, the CheR to pentapeptide-bearing receptor (PP_{MCPs}) ratio is particularly high in *S. meliloti* with approximately five CheR molecules per PP_{MCPs} monomer, compared to 0.01 in *E. coli* (Arapov et al., 2020). Lastly, the presence of CheD and the interaction between CheT and CheR described in this work sets the *S. meliloti* system apart from the enterobacterial paradigm.

Phosphorylation assays with CheA~^{32}P, CheA~^{32}P/CheS, CheY1, and CheT at molar ratios of 0.5:1:0.1 revealed a two-fold increase in CheY1~P dephosphorylation by CheT. An effect of CheS on CheT function is unlikely as dephosphorylation of CheY1 by CheT was unchanged in the presence of CheS (Figure 3c). CheT variant proteins with substitutions in the phosphatase motif had no effect on CheY1 dephosphorylation (Figure 4c,f). CheT binds CheY1-BeF_3^- 25-fold more strongly than unphosphorylated CheY1, and this binding is partly dependent on the DXXXQ phosphatase motif as substitution of Asp to Ala increased binding to CheY1 and decreased binding to CheY1-BeF_3^- (Figure 5c,d). In comparison, *E. coli* CheZ binds to CheY~P 26-fold more strongly than to unphosphorylated CheY (Blat & Eisenbach, 1994). The formation of homodimers is another characteristic CheT shares with CheZ (Blat & Eisenbach, 1996b) (Figure 8a). These findings position CheT as a typical chemotaxis response regulator phosphatase but also as a novel player in the signal termination pathway of *S. meliloti*.

This pathway was previously thought to lack a phosphatase and instead solely uses a phosphate sink for signal termination (Figures 3b and 4) (Dogra et al., 2012; Schmitt, 2002; Sourjik & Schmitt, 1998). An intriguing preference of CheT binding and enzymatic activity towards CheY1 but not CheY2 can be reasoned by the relatively low identity of only 37% for the 120 amino acid residues that form the ordered $(\beta/\alpha)_5$ domain (Figure S3). In the previously determined structure of CheY2 bound to the phosphomimetic BeF_3^-, (PDB ID 1P6U) (Riepl et al., 2004), the side chains of 66 residues in the globular domain present >25% solvent accessible surface area. Of these exposed side chains, 22 (33%) are identical between CheY1 and CheY2, slightly lower than the 41% identity of the 54 buried residues. The relatively low conservation of surface residues in CheY1 and CheY2 are consistent with the observed differences in interactions of these two response regulators with partner proteins that underlie their distinct roles in chemotactic signaling.

Since CheY1 serves as a sink towards the motor output response regulator, enhanced CheY1~P dephosphorylation should allow for a better drainage of the phosphoryl group pool (Amin et al., 2014; Dogra et al., 2012). In this case, the expected motility phenotype of a strain lacking the CheY1 phosphatase would be a reduction in swimming speed, as CheY2~P levels would be increased. However, the deletion of *cheT* or the introduction of point mutations in the DXXXQ phosphatase motif resulted in increased swimming velocities of these mutants pointing to a decreased cellular concentration of CheY2~P (Figure 6b). The high swimming speeds in the *cheT* mutants relative to wild type appear to be a consequence of increased cellular levels of CheY1~P in the absence of CheT or its phosphatase activity. Since phosphotransfer from CheA~P to CheY2 is reversible and in equilibrium, the effectual CheY2~P levels are a consequence of a shift toward the formation of CheY1~P (Sourjik & Schmitt, 1998). Thus, high cellular levels of CheY1~P might have an inhibitory effect on kinase activity, which would reduce cellular levels of CheY2~P and lead to an increase in swimming speed. Alternatively, it is plausible that high levels of CheY1~P led to a redirection of phosphoryl groups from CheA~P to CheB, thus increasing CheB~P levels and its inhibitory action on CheA kinase activity. Consequently, CheY2~P levels decrease and the swimming speed increases.

Interestingly, *cheT* phosphatase mutants increased their swimming velocity upon attractant stimulation, a phenotype that is not shared with the *cheT* deletion mutant (Figure 6b). This implies that elimination of CheT's phosphatase activity only affects its function on CheY1 but not its other role(s) in *S. meliloti* chemotaxis. On the contrary, deletion of *cheT* negatively affected the cellular response to the attractant proline, a feature that was also observed in the *cheR* deletion strain (Figure 6b). Furthermore, both phosphatase motif mutants presented a swim ring diameter that was two-thirds of the wild-type swim ring and similar to that of the *cheY1* deletion strain. On the other hand, the swim ring diameter of the *cheT* deletion strain was half of the wild-type swim ring (Figure S1). This further implies that CheT, in addition to its phosphatase activity on CheY1~P, exerts another function in *S. meliloti* chemotaxis. This second function is likely taking part in the adaptation process.

We discovered that CheT interacts with the methyltransferase CheR with a K_D of 19 μM as monitored by ITC experiments (Figure 7a,b). SEC-MALS experiments indicated that CheT monomers and dimers are capable of complex formation with CheR monomers (Figure 8c). The close interaction between CheT and CheR motivated us to investigate whether they affect each other's function. However, CheR had no effect on the phosphatase activity of CheT, and CheT had no effect on the methylation of McpX by CheR (Figures 9–11). It remains to be seen whether CheT affects the methyltransferase activity of CheR with other MCPs. Meanwhile, evidence in this study indicates that CheT most likely also plays a role in chemotactic adaptation, as CheR and CheT form a stable complex and mutants lacking either *cheR* or *cheT* present similar characteristics in swim speed assays.

The *S. meliloti* CheT-CheR-CheY1~P interaction resembles the CheC-CheD-CheY~P adaptation system in *Bacillus subtilis* as both systems consist of a phosphatase (CheC), an adaptation protein (CheD), and a phosphorylated response regulator (CheY~P). CheC binds to both CheD and CheY~P, which is analogous to the CheT interaction with CheR and CheY1~P. While *S. meliloti* CheR has no effect on the activity of CheT and vice versa, binding of CheD to CheC increases the phosphatase activity on CheY~P by approximately five-fold in *B. subtilis* (Chao et al., 2006; Muff & Ordal, 2007; Szurmant et al., 2004). Furthermore, the behavior of strains expressing CheC variants with disrupted CheY interaction or abolished phosphatase activity demonstrates that chemotaxis is largely dependent on CheC binding to CheY~P and CheD rather than on its CheY~P phosphatase activity (Muff & Ordal, 2007). Ongoing research aims to identify CheT residues required for CheR and CheY1~P binding, an important step to further characterize the role of CheT in *S. meliloti* chemotaxis.

Here, we have shown that CheT is part of the signal termination and adaptation system of *S. meliloti* chemotaxis, which was a rather unexpected result. More insights can be gained by investigating the unexplored functions of chemoreceptor methylation and demethylation by CheR and CheB, respectively, and the role of CheD in adaptation.

4 | MATERIALS AND METHODS

4.1 | Bacterial strains and plasmids

E. coli K12 and *S. meliloti* MV II-I derivatives used are listed in Table 1. The wild-type *S. meliloti* strain RU11/001, is a spontaneous streptomycin-resistant derivative of MVII-1 (Krupski et al., 1985).

4.2 | Genetic and DNA manipulations

S. meliloti mutants listed in Table 1 were created by allelic replacement essentially as laid out in Sourjik and Schmitt (1996) and Zatakia et al. (2018).

4.3 | Media and growth conditions

S. meliloti strains were grown in TYC (0.5% (wt/vol) tryptone, 0.3% (wt/vol) yeast extract, 0.13% (wt/vol) $CaCl_2 \times 6\ H_2O$ [pH 7.0]) at 30°C for 2 days. For motility and tracking experiments, cultures were subsequently diluted 1:100 in 10 mL RB minimal medium [6.1 mM K_2HPO_4, 3.9 mM KH_2PO_4, 1 mM $MgSO_4$, 1 mM $(NH_4)_2SO_4$, 0.1 mM $CaCl_2$, 0.1 mM NaCl, 0.01 mM Na_2MoO_4, 0.001 mM $FeSO_4$, 20 μg/L biotin, 100 μg/L thiamine], which was added as liquid layer on top of Bromfield medium (0.04% (wt/vol) tryptone, 0.01% (wt/vol) yeast extract, 0.01% (wt/vol) $CaCl_2{\cdot}2H_2O$) agar plates and incubated at 30°C to an optical density at 600 nm (OD_{600}) of 0.1. *E. coli* strains were grown at 37°C in lysogeny broth (LB). Antibiotics were used at the following concentration: for *S. meliloti*, streptomycin at 600 μg/mL, neomycin 120 μg/mL, for *E. coli*, ampicillin at 100 μg/mL and chloramphenicol at 30 μg/mL.

4.4 | Swim plate assays

Bromfield medium swim plates containing 0.3% (wt/vol) Bacto agar were inoculated with 3 μL of *S. meliloti* cultures grown in TYC and incubated at 30°C for 3–4 days.

4.5 | Computerized motion analysis of free-swimming cells

Overnight cultures were grown to an OD_{600} of 2.5 and diluted to OD_{600} of 0.004 in an overlay broth that was prepared by

TABLE 1 Bacterial strains and plasmids.

Strain/plasmid	Relevant characteristics	Source or reference
E. coli		
BL21(DE3)	*F− ompT hsdSB(rB− mB−) gal dcm λ (DE3)*	Novagen
ER2566	*ion ompT lacZ::T7*	New England Biolabs
Lemo21(DE3)	*fhuA2 [lon] ompT gal* (λDE3) *dcm ΔhsdS*/pLemo(Cm^r)	New England Biolabs
M15/pREP4	Ap^r Km^r; F- ϕ80ΔlacM15 *thi lac- mtl- recA*$^+$	Qiagen
S17-1	Sm^r Tp^r; *recA endA thi hsdR* RP4-2 Tc::Mu::Tn7	Simon et al. (1986)
S. meliloti		
RU11/001	Sm^r; Spontaneous streptomycin-resistant wild-type strain	Pleier and Schmitt (1991)
RU11/306	Δ*cheR*	Arapov et al. 2020
RU11/307	Δ*cheY2*	Sourjik and Schmitt (1996)
RU11/308	Δ*cheY1*	Sourjik and Schmitt (1996)
RU11/310	Δ*cheA*	Sourjik and Schmitt (1996)
RU11/312	Δ*cheB*	Arapov et al. (2020)
RU11/319	Δ*cheT*	Arapov et al. (2020)
RU11/411	Δ*cheD*	Arapov et al. (2020)
BS170	Sm^r; *cheT* with codon 61 changed from CAG to GCC (Q61A)	This study
BS190	Sm^r; *cheT* with codon 57 changed from GAC to GCC (D57A)	This study
BS192	Sm^r; *cheT* with codon 57 changed from GAC to GCC (D57A) & codon 61 changed from CAG to GCC (Q61A)	This study
Plasmids		
pBBR1-MCS2	Km^r; broad host-range vector	Kovach et al. (1995)
pBS16[a]	Ap^r; pTYB1-*cheY1*	Riepl et al. (2008)
pBS18[a]	Ap^r; pTYB1-*cheY2*	Riepl et al. (2008)
pBS54	Ap^r; pTYB11-*motB*	Sobe et al. (2022)
pBS57[a]	Ap^r; pTYB1-*cheA*	Riepl et al. (2008)
pBS93	Ap^r; pTYB11-*cheB*	This study
pBS173	Km^r; 291-bp NcoI-BamHI fragment from pRU2804 containing *cheS* cloned into pET27bmod	Dogra et al. (2012)
pBS189	Km^r; pBBR1MCS2-*lacI*^{q}	Webb et al. (2014)
pBS295	Km^r; pET27bmod-*cheA*-6Xhistag	Dogra et al. (2012)
pBS331	Ap^r; pTYB11-*cheD*	This study
pBS359	Ap^r; pTYB11-*cheT*	This study

(Continues)

TABLE 1 (Continued)

Strain/plasmid	Relevant characteristics	Source or reference
pBS445	Km^r; pBS189-*cheT*	This study
pBS450	Ap^r; pTYB1-*cheR*	This study
pBS567	Ap^r; pQE60-*cheW1*	This study
pBS639	Ap^r; pTYB11-CheTD57A	This study
pBS667	Ap^r; pTYB11-CheTQ61A	This study
pBS1095	Ap^r; pET22B(+)-*mcpU*	This study
pBS1096	Ap^r; pET22B(+)-*mcpX*	This study
pET27bmod	Km^r; expression vector	Novagen
pK18*mobsacB*	Km^r; *mob sacB*, vector used for homologous allelic exchange	Schäfer et al. (1994)
pQE60	Ap^r	Qiagen
pTYB1	Ap^r; expression vector for Impact system	New England Biolabs
pTYB11	Ap^r; expression vector for Impact system	New England Biolabs

[a]Equivalent to pRU2312, pRU2313, and pRU2326, respectively, as described in Riepl et al. (2008).

incubating Bromfield plates with a 10-ml layer of RB at 30°C for 16 h. Motile cells between an OD_{600} of 0.16–0.18 were harvested and suspended in RB to a final OD_{600} of 0.05 (Sobe et al., 2022). To determine swimming velocities, bacteria were analyzed by phase-contrast microscopy using a Nikon Eclipse E600 microscope with a 40× objective and a custom Nikon CMOS camera from The Imaging Source or a Zeiss standard 14 phase-contrast microscope (magnification, ×400) (Charlotte, NC, USA). After addition of 10 mM proline to cultures on a slide, videos of the motile behavior of wild-type and mutant cell populations were taken within 20 s. Five-second videos were analyzed using the TumbleScore program to quantify swimming velocities (Pottash et al., 2017) or swim tracks were analyzed using the computerized motion analysis of the Hobson BacTracker system (Hobson Tracking Systems, Sheffield, United Kingdom) as previously described in Meier et al. (2007). Mean and standard deviation were calculated from three separate biological replicates. Statistical significance was determined by a two-tailed Student's *T-test* in relation to the wild-type strain speed.

4.6 | Expression and purification of CheR and CheT

CheT and CheR were overexpressed in *E. coli* ER2566 from pBS359 and pBS450, respectively. Cells were grown at 37°C in LB containing 100 μg/mL ampicillin to an OD_{600} of 0.7–0.9 and gene expression was induced with 0.3 mM IPTG (isopropyl-β-d-thiogalactopyranoside). Cultivation of the cells continued for 16–20 h at 16°C until cells harvest by centrifugation. The cells were suspended in IMPACT buffer (20 mM Tris/HCl [pH 8.0], 500 mM NaCl, 1 mM EDTA). Cells were then lysed by three passages through a French pressure cell (SLM Aminco, Silver Spring, MD) at 20,000 psi and centrifuged 48,000×*g* at 4°C for 1 h to remove insoluble material and unlysed cells. The soluble fraction was passed through a 0.2-μm filter and loaded on a chitin agarose (NE Biolabs, Beverly MA, USA) column (2.6 × 5.0 cm) equilibrated with IMPACT buffer. The column was washed with 10–20 bed volumes of IMPACT buffer at 4°C. Intein-mediated cleavage was induced by equilibration of the column with two bed volumes of IMPACT buffer containing 50 mM dithiothreitol, followed by 12–36 h incubation at 4°C. The protein was eluted with IMPACT buffer and protein-containing fractions were collected. Fractions were pooled, concentrated to 10 mL and subjected to size exclusion chromatography (SEC) on a HiPrep™ 26/60 Sephacryl™ S-200 HR column (GE Healthcare Life Sciences). Cells were grown at 37°C in lysogeny broth (LB) containing 100 μg/mL ampicillin to an OD_{600} of 0.7–0.9 and gene expression was induced with 0.5 mM IPTG. Cultivation of the cells continued for 4 h at 37°C until cells harvest by centrifugation. Cells were suspended in Ni-NTA binding buffer (500 mM NaCl, 20 mM imidazole, 1 mM PMSF, 20 mM $NaPO_4$ [pH 7.0]), lysed by three passages through a French pressure cell (SLM Aminco, Silver Spring, MD), and centrifuged for 1 h at 48,000×*g* and 4°C. The soluble fraction was passed through a 0.2-μm filter and loaded onto a charged 5-ml Ni-NTA column (GE Healthcare Life Sciences). Proteins were eluted using a linear gradient of elution buffer (500 mM NaCl, 500 mM imidazole, 1 mM PMSF, 20 mM $NaPO_4$ [pH 7.0]). Protein-containing elution fractions were pooled, concentrated and further purified through SEC on a HiPrep 26/60 Sephacryl™ S-200 HR column (Cytiva).

4.7 | Expression and purification of other chemotaxis proteins

Expression and purification of CheA, CheA/CheS complex, CheY1, CheY2, and CheS was performed as described in Dogra et al. (2012). Expression and purification of CheB, CheD, and CheW1 was accomplished essentially as described in Arapov et al. (2020).

4.8 | Size exclusion chromatography and multiangle light scattering

The molecular masses of CheT, CheR, CheT/CheR, and CheY1 were determined by size exclusion chromatography with online absorbance, multiangle light scattering (MiniDawn, Wyatt Technology), and refractive index detectors (Optilab). One milligram of purified proteins and CheR and CheT mixture were incubated at room temperature for 30 min before being subjected to Superdex 200 increase (10/300 GL) column (Cytiva), which was equilibrated in 25 mM Tris/HCl pH 7.5, 125 mM NaCl at 22°C and a flow rate of 0.5 mL/min. The refractive index (RI) signal was used as a concentration source for analyzing the light scattering data with the ASTRA program (version 8.1.2.1; Wyatt Technology).

4.9 | Isothermal titration calorimetry

Direct binding analysis was performed with a MicroCal PEAQ-ITC (Malvern Panalytical Ltd). Three hundred microliters of 30–50 μM CheR or CheY1/CheY1-BeF_3^- were loaded into the sample cell and titrated with 300–535 μM of CheT from the syringe. To produce the CheY1-BeF_3^- complex, 7 mM $MgCl_2$, 5 mM $BeSO_4$, and 30 mM NaF were mixed with 30–50 μM CheY1 for 5 min at room temperature. All ITC experiments were performed at 25°C. Protein solutions were degassed at 24°C before loading them into the MicroCal PEAQ-ITC. To obtain baseline titrations and for reference subtraction, proteins were titrated into buffer only. The dissociation constant (K_D) was determined from heat changes during titration of the ligand with the protein using the MicroCal PEAQ-ITC analysis software "one binding sites" model.

4.10 | In-vitro crosslinking assays

Freshly prepared glutaraldehyde (Sigma-Aldrich) at a final concentration of 1% (wt/vol) was used for protein crosslinking experiments essentially as previously described (Riepl et al., 2008). Proteins were used at a concentration of 0.7 μM in a buffer containing 20 mM NaCl, 1 mM EDTA, 20 mM $NaPO_4$, pH 7.5. Reactions were stopped after an incubation of 30 min at room temperature by the addition of an equal volume of 2× Laemmli buffer.

4.11 | Immunoblots

Cross-linked samples were separated by gel electrophoresis on a 15% SDS polyacrylamide gel and transferred to a 0.45-μm nitrocellulose membrane in transfer buffer (20% (vol/vol) methanol, 50 mM Tris, 40 mM glycine). Membranes were blocked overnight with 5% (wt/vol) non-fat dry milk with 0.1% (vol/vol) Tween 20 in phosphate-buffered saline (PBS, 100 mM NaCl, 80 mM Na_2HPO_4, 20 mM NaH_2PO_4, pH 7.5). Blots were then probed with anti-CheT or anti-CheR affinity-purified antibodies at a 1:400 dilution for 1.5 h at room temperature. Blots were subsequently washed for 30 min with PBS/0.1% Tween 20 with four buffer changes and probed with donkey anti-rabbit conjugated with horseradish peroxidase at a 1:1500 dilution for 1.5 h. The blots were then washed for 30 min with PBS/0.1% Tween 20 with four buffer changes. Detection was performed by chemiluminescence (Amersham ECL Western Blotting Detection Kit, GE Healthcare) using Hyperfilm ECL (GE Healthcare).

4.12 | Autophosphorylation of CheA and phosphotransfer to CheY1 or CheY2 in the presence of CheT

Purified CheA and CheA/CheS complex was dialyzed against 20 mM Tris/HCl, pH 7.5, 0.5 mM EDTA, 2 mM DTT, 10% (vol/vol) glycerol ($TEDG_{10}$) overnight at 4°C. Autophosphorylation was initiated by the addition of 0.6 mM 10 μCi [γ-^{32}P] ATP. Reactions were performed in $TEDG_{10}$ containing 5 mM $MgCl_2$ and 50 mM KCl at a final CheA concentration of 5 μM at 22°C. Phosphotransfer was initiated by the addition of 25 μM CheY2 or CheY1 and monitored in the presence of 50 μM of CheT or CheT variants. Phosphorylation was terminated at given time intervals by adding 10-μl aliquots of the reaction mixture to 10 μL of SDS gel-loading buffer containing 10 mM EDTA. Samples were separated by electrophoresis on a 4%–20% Criterion TGX gradient gel (Biorad). Gels were enclosed in plastic wrap and exposed to a storage phosphor screen which was excited with a 633-nm excitation laser and observed using a 390-nm band filter using Amersham Typhoon phosphorimager (Cytiva). Band intensities were quantified with ImageQuant TL software (Cytiva).

4.13 | Purification of [^{32}P]-phospho-CheA

Purified CheA and CheA/CheS complex (6.1 nmol each) was phosphorylated in 500 μL $TEDG_{10}$ containing 5 mM $MgCl_2$ and 50 mM KCl using 100 μCi of 0.4 mM [γ-^{32}P]-ATP for 15 min at 22°C. The reaction mixture was subjected to gel filtration on a Sephadex G-50 column (16/20; Pharmacia Biotech) at a flow rate of 0.5 mL/min. The column was developed and equilibrated in $TEDG_{10}$, protein-containing fractions were combined after subjected to Liquid Scintillation Counting, and stored at −20°C. According to quantitative protein assays and scintillation counting, approximately 5% of CheA was phosphorylated.

4.14 | Kinetic assays of phosphotransfer from [^{32}P] phospho-CheA and [^{32}P]phospho-CheAS complex to CheY1 and phosphatase activity of CheT and CheT/CheT mixtures

Phosphotransfer reactions from purified [^{32}P]phospho-CheA and [^{32}P]phospho-CheA/CheS complex (400 nM) were initiated by the addition of CheY1 or CheY2 (40 nM) in $TEDG_{10}$ containing 5 mM $MgCl_2$ and 50 mM KCl and phosphatase activity of CheT was assayed by adding 4 nM of CheT, CheT variants, and CheT/CheR mixtures after incubation for 30 min at room temperature. Reactions were terminated at given time intervals by adding 10-μL aliquots of the reaction mixture to 10 μL of SDS gel loading buffer containing 10 mM EDTA. Samples were separated by electrophoresis on a 4%–20% Criterion TGX gradient gel (Biorad) and analyzed. Gels were enclosed in plastic wrap and exposed to a storage phosphor screen which was Amersham Typhoon phosphorimager (Cytiva). Band intensities were quantified with ImageQuant TL software (Cytiva), and time courses were plotted using Origin 8.1 software (OriginLab, Northampton, MA).

4.15 | Isolation of McpX-containing membrane vesicles

Preparation of membrane vesicles was done essentially as previously described in Osborne and Munson (1974) and Gegner et al. (1992).

An overnight culture of *E. coli* Lemo21(DE3) with pBS1096 expressing McpX grown in LB containing ampicillin and chloramphenicol as well as 500 μM L-rhamnose was diluted to a final OD_{600} of 0.05. To ensure proper aeration, cultures were placed in flasks with the volume of the growth medium not exceeding 15% of the maximum volume of each flask. Cells were grown at 37°C to an OD_{600} of 0.4–0.5, gene expression was induced by 0.4 mM IPTG and cultivation continued for 4 h at 37°C. Cells were harvested by centrifugation and suspended in 10 mM Tris/HCl (pH 7.5), 20% sucrose (wt/wt). Lysozyme and EDTA were subsequently added to a final concentration of 100 μg/mL and 5 mM, respectively. Cells were incubated on ice for 5 min under gentle agitation. Two volumes of 5 mM EDTA, 1 mM PMSF and 1 mM 1,10 phenanthroline (Phe) were then slowly added with a glass pipette. Cells were lysed by the addition of four volumes of ice-cold H_2O and subsequent vigorous agitation for 1 min. DNase and $MgCl_2$ were added to a final concentration of 10 μg/mL and 3 mM, respectively. The lysate was centrifuged for 1.5 h at 27,485×*g* and 4°C. The insoluble fraction was suspended in 50 mM Tris/HCl [pH 7.5], 5 mM $MgCl_2$, 50 mM KCl, 0.5 mM PMSF, 1 mM Phe, and subsequently dialyzed for 14 h at 4°C against the same buffer.

4.16 | In-vitro methylation assays

In-vitro methylation assays were carried out essentially as described in Barnakov et al. (1998). Isolated membrane vesicles with and without McpX, CheT, and CheR were dialyzed against TGD buffer (50 mM Tris/HCl [pH 7.5], 10% (v/v) glycerol, 5 mM dithiothreitol). McpX in membrane vesicles and CheR were used at 1.2 and 0.2 μM, respectively, in the absence and in the presence of 4.6 μM CheT, and reactions were initiated by addition of adenosyl-L-methionine S-[methyl-^{3}H] (SAM) (PerkinElmer) (0.9 Ci/mmol) at a final concentration of 50 μM. At indicated time points, 20-μl samples were added to 20 μL 2× Laemmli buffer and boiled for 1 min to terminate the reactions. Twenty-microliter aliquots were analyzed by electrophoresis on a 10% acrylamide SDS-gel. Bands corresponding to McpX were excised from Coomassie-stained dry gels. The excised bands were subjected to alkali hydrolysis in 200 μL 1 M NaOH for 24 h. Quantification of released radiolabeled methanol was enabled by vapor-phase equilibrium of volatile methanol and ECONO-SAFE scintillation cocktail.

AUTHOR CONTRIBUTIONS

Alfred Agbekudzi: Investigation; writing – original draft; methodology; validation; visualization; writing – review and editing; formal analysis; data curation. **Timofey D. Arapov:** Investigation; writing – original draft; methodology; validation; writing – review and editing; visualization; formal analysis; data curation. **Ann M. Stock:** Conceptualization; methodology; project administration; resources. **Birgit E. Scharf:** Conceptualization; investigation; funding acquisition; writing – review and editing; methodology; validation; project administration; supervision; resources.

ACKNOWLEDGMENTS

This study was supported by NSF grants MCB-1253234 and MCB-1817652 to B.E.S. We are indebted to Dr. Gerald L. Hazelbauer (University of Missouri) for his generosity in hosting T.D.A. in his laboratory to acquire knowledge, training, and advice about membrane vesicle purification and in-vitro methylation assays, and to Dr. Wing-Cheung Lai for his patience in training T.D.A. in these techniques. We would like to thank Andrea Brücher for motility measurements, Victor Sourjik for constructing strains RU11/306, RU11/312, RU11/319, and Paul Muschler for constructing strain RU11/411 (Department of Genetics, University Regensburg, Germany).

DATA AVAILABILITY STATEMENT

The data that support the findings of this study are available on request from the corresponding author. The data are not publicly available due to privacy or ethical restrictions.

ETHICS STATEMENT

No human or animal subjects were used in this work.

ORCID

Birgit E. Scharf https://orcid.org/0000-0001-6271-8972

REFERENCES

Agbekudzi, A. & Scharf, B.E. (2024) Chemoreceptors in *Sinorhizobium meliloti* require minimal pentapeptide tethers to provide adaptational assistance. *Molecular Microbiology*, 122(1), 50–67.

Amin, M., Kothamachu, V.B., Feliu, E., Scharf, B.E., Porter, S.L. & Soyer, O.S. (2014) Phosphate sink containing two-component signaling systems as tunable threshold devices. *PLoS Computational Biology*, 10(10), e1003890.

Arapov, T.D. et al. (2020) Cellular stoichiometry of chemotaxis proteins in Sinorhizobium meliloti. *Journal of Bacteriology*, 202(14), e00141-20.

Ashish, C. (2015) *Sinorhizobium meliloti* bacteria contributing to rehabilitate the toxic environment. *Journal of Bioremediation & Biodegradation*, 6(2), 1–2.

Attmannspacher, U., Scharf, B. & Schmitt, R. (2005) Control of speed modulation (chemokinesis) in the unidirectional rotary motor of *Sinorhizobium meliloti*. *Molecular Microbiology*, 56(3), 708–18.

Baaziz, H., Compton, K.K., Hildreth, S.B., Helm, R.F. & Scharf, B.E. (2021) McpT, a broad-range carboxylate chemoreceptor in *Sinorhizobium meliloti*. *Journal of Bacteriology*, 203(17), e00216-21.

Barnakov, A.N., Barnakova, L.A. & Hazelbauer, G.L. (1998) Comparison in vitro of a high-and a low-abundance chemoreceptor of *Escherichia coli*: similar kinase activation but different methyl-accepting activities. *Journal of Bacteriology*, 180(24), 6713–18.

Barnakov, A.N., Barnakova, L.A. & Hazelbauer, G.L. (1999) Efficient adaptational demethylation of chemoreceptors requires the same enzyme-docking site as efficient methylation. *Proceedings of the National Academy of Sciences*, 96(19), 10667–0672.

Berg, H.C. (1993) *Random walks in biology*. Princeton, NJ: Princeton University Press.

Bischoff, D.S. & Ordal, G.W. (1992) Identification and characterization of FliY, a novel component of the *Bacillus subtilis* flagellar switch complex. *Molecular Microbiology*, 6(18), 2715–23.

Blat, Y. & Eisenbach, M. (1994) Phosphorylation-dependent binding of the chemotaxis signal molecule CheY to its phosphatase, CheZ. *Biochemistry*, 33(4), 902–6.

Blat, Y. & Eisenbach, M. (1996a) Mutants with defective phosphatase activity show no phosphorylation-dependent oligomerization of CheZ: the phosphatase of bacterial chemotaxis (*). *Journal of Biological Chemistry*, 271(2), 1232–6.

Blat, Y. & Eisenbach, M. (1996b) Oligomerization of THE phosphatase CheZ upon interaction with the phosphorylated form of CheY: the signal protein of bacterial chemotaxis (*). *Journal of Biological Chemistry*, 271(2), 1226–31.

Borkovich, K.A., Kaplan, N., Hess, J.F. & Simon, M.I. (1989) Transmembrane signal transduction in bacterial chemotaxis involves ligand-dependent activation of phosphate group transfer. *Proceedings of the National Academy of Sciences*, 86(4), 1208–12.

Bourret, R.B., Borkovich, K.A. & Simon, M.I. (1991) Signal transduction pathways involving protein phosphorylation in prokaryotes. *Annual Review of Biochemistry*, 60(1), 401–41.

Briegel, A., Ladinsky, M.S., Oikonomou, C., Jones, C.W., Harris, M.J., Fowler, D.J. et al. (2014) Structure of bacterial cytoplasmic chemoreceptor arrays and implications for chemotactic signaling. *eLife*, 3, e02151.

Chao, X., Muff, T.J., Park, S.Y., Zhang, S., Pollard, A.M., Ordal, G.W. et al. (2006) A receptor-modifying deamidase in complex with a signaling phosphatase reveals reciprocal regulation. *Cell*, 124(3), 561–71.

Compton, K.K., Hildreth, S.B., Helm, R.F. & Scharf, B.E. (2018) *Sinorhizobium meliloti* chemoreceptor McpV senses short-chain carboxylates via direct binding. *Journal of Bacteriology*, 200(23), e00519-18.

Djordjevic, S. & Stock, A.M. (1998) Structural analysis of bacterial chemotaxis proteins: components of a dynamic signaling system. *Journal of Structural Biology*, 124(2–3), 189–200.

Dogra, G., Purschke, F.G., Wagner, V., Haslbeck, M., Kriehuber, T., Hughes, J.G. et al. (2012) *Sinorhizobium meliloti* CheA complexed with CheS exhibits enhanced binding to CheY1, resulting in accelerated CheY1 dephosphorylation. *Journal of Bacteriology*, 194(5), 1075–87.

Erhardt, M. (2016) Strategies to block bacterial pathogenesis by interference with motility and chemotaxis. In: Stadler, M. & Dersch, P. (Eds.) *How to overcome the antibiotic crisis: facts, challenges, technologies and future perspectives*. Cham: Springer International Publishing, pp. 185–205.

Gage, D.J. (2004) Infection and invasion of roots by symbiotic, nitrogen-fixing rhizobia during nodulation of temperate legumes. *Microbiology and Molecular Biology Reviews*, 68(2), 280–300.

Garrity, L.F. & Ordal, G.W. (1995) Chemotaxis in *Bacillus subtilis*: how bacteria monitor environmental signals. *Pharmacology & Therapeutics*, 68(1), 87–104.

Garrity, L.F. & Ordal, G.W. (1997) Activation of the CheA kinase by asparagine in *Bacillus subtilis* chemotaxis. *Microbiology*, 143(9), 2945–51.

Gegner, J.A., Graham, D.R., Roth, A.F. & Dahlquist, F.W. (1992) Assembly of an MCP receptor, CheW, and kinase CheA complex in the bacterial chemotaxis signal transduction pathway. *Cell*, 70(6), 975–82.

Glekas, G.D., Cates, J.R., Cohen, T.M., Rao, C.V. & Ordal, G.W. (2011) Site-specific methylation in *Bacillus subtilis* chemotaxis: effect of covalent modifications to the chemotaxis receptor McpB. *Microbiology*, 157(Pt 1), 56–65.

Götz, R. & Schmitt, R. (1987) Rhizobium meliloti swims by unidirectional, intermittent rotation of right-handed flagellar helices. *Journal of Bacteriology*, 169(7), 3146–50.

Hazelbauer, G.L., Falke, J.J. & Parkinson, J.S. (2008) Bacterial chemoreceptors: high-performance signaling in networked arrays. *Trends in Biochemical Sciences*, 33(1), 9–19.

Hess, J.F., Oosawa, K., Kaplan, N. & Simon, M.I. (1988) Phosphorylation of three proteins in the signaling pathway of bacterial chemotaxis. *Cell*, 53(1), 79–87.

Kehry, M.R., Bond, M.W., Hunkapiller, M.W. & Dahlquist, F.W. (1983) Enzymatic deamidation of methyl-accepting chemotaxis proteins in *Escherichia coli* catalyzed by the cheB gene product. *Proceedings of the National Academy of Sciences*, 80(12), 3599–3603.

Kovach, M.E., Elzer, P.H., Steven Hill, D., Robertson, G.T., Farris, M.A., Roop, R.M., II et al. (1995) Four new derivatives of the broad-host-range cloning vector pBBR1MCS, carrying different antibiotic-resistance cassettes. *Gene*, 166(1), 175–6.

Krembel, A., Colin, R. & Sourjik, V. (2015) Importance of multiple methylation sites in *Escherichia coli* chemotaxis. *PLoS ONE*, 10(12), e0145582.

Kristich, C.J. & Ordal, G.W. (2002) Bacillus subtilis CheD is a chemoreceptor modification enzyme required for chemotaxis. *Journal of Biological Chemistry*, 277(28), 25356–5362.

Krupski, G., Götz, R., Ober, K., Pleier, E. & Schmitt, R. (1985) Structure of complex flagellar filaments in *Rhizobium meliloti*. *Journal of Bacteriology*, 162(1), 361–6.

Lai, W.-C., Barnakova, L.A., Barnakov, A.N. & Hazelbauer, G.L. (2006) Similarities and differences in interactions of the activity-enhancing chemoreceptor pentapeptide with the two enzymes of adaptational modification. *Journal of Bacteriology*, 188(15), 5646–9.

Levit, M.N., Liu, Y. & Stock, J.B. (1999) Mechanism of CheA protein kinase activation in receptor signaling complexes. *Biochemistry*, 38(20), 6651–8.

Liu, X., Liu, W., Sun, Y., Xia, C., Elmerich, C. & Xie, Z. (2018) A cheZ-like gene in *Azorhizobium caulinodans* is a key gene in the control of chemotaxis and colonization of the host plant. *Applied and Environmental Microbiology*, 84(3), e01827-17.

Lukat, G.S., Lee, B.H., Mottonen, J.M., Stock, A.M. & Stock, J.B. (1991) Roles of the highly conserved aspartate and lysine residues in the response regulator of bacterial chemotaxis. *Journal of Biological Chemistry*, 266(13), 8348–54.

Meier, V.M., Muschler, P. & Scharf, B.E. (2007) Functional analysis of nine putative chemoreceptor proteins in *Sinorhizobium meliloti*. *Journal of Bacteriology*, 189(5), 1816–26.

Miller, L.D., Russell, M.H. & Alexandre, G. (2009) Diversity in bacterial chemotactic responses and niche adaptation. *Advances in Applied Microbiology*, 66, 53–75.

Morgan, D., Baumgartner, J. & Hazelbauer, G. (1993) Proteins antigenically related to methyl-accepting chemotaxis proteins of *Escherichia coli* detected in a wide range of bacterial species. *Journal of Bacteriology*, 175(1), 133–40.

Muff, T.J. & Ordal, G.W. (2007) The CheC phosphatase regulates chemotactic adaptation through CheD. *Journal of Biological Chemistry*, 282(47), 34120–4128.

Orr, M.W. & Lee, V.T. (2016) A PilZ domain protein for chemotaxis adds another layer to c-di-GMP–mediated regulation of flagellar motility. *Science Signaling*, 9(450), fs16.

Osborn, M. & Munson, R. (1974) [67] Separation of the inner (cytoplasmic) and outer membranes of gram-negative bacteria. In: *Methods in enzymology*. New York: Academic Press, pp. 642–53.

Parkinson, J.S., Ames, P. & Studdert, C.A. (2005) Collaborative signaling by bacterial chemoreceptors. *Current Opinion in Microbiology*, 8(2), 116–21.

Perez, E. & Stock, A.M. (2007) Characterization of the *Thermotoga maritima* chemotaxis methylation system that lacks pentapeptide-dependent methyltransferase CheR:MCP tethering. *Molecular Microbiology*, 63(2), 363–78.

Pleier, E. & Schmitt, R. (1991) Expression of two *Rhizobium meliloti* flagellin genes and their contribution to the complex filament structure. *Journal of Bacteriology*, 173(6), 2077–85.

Porter, S.L., Wadhams, G.H. & Armitage, J.P. (2011) Signal processing in complex chemotaxis pathways. *Nature Reviews Microbiology*, 9(3), 153–65.

Pottash, A.E., McKay, R., Virgile, C.R., Ueda, H. & Bentley, W.E. (2017) TumbleScore: run and tumble analysis for low frame-rate motility videos. *BioTechniques*, 62(1), 31–36.

Rao, C.V., Glekas, G.D. & Ordal, G.W. (2008) The three adaptation systems of *Bacillus subtilis* chemotaxis. *Trends in Microbiology*, 16(10), 480–7.

Riepl, H., Maurer, T., Kalbitzer, H.R., Meier, V.M., Haslbeck, M., Schmitt, R. et al. (2008) Interaction of CheY2 and CheY2-P with the cognate

CheA kinase in the chemosensory-signalling chain of *Sinorhizobium meliloti*. *Molecular Microbiology*, 69(6), 1373–84.
Riepl, H., Scharf, B., Schmitt, R., Kalbitzer, H.R. & Maurer, T. (2004) Solution structures of the inactive and BeF3-activated response regulator CheY2. *Journal of Molecular Biology*, 338(2), 287–97.
Rosario, M.M.L. & Ordal, G.W. (1996) CheC and CheD interact to regulate methylation of *Bacillus subtilis* methyl-accepting chemotaxis proteins. *Molecular Microbiology*, 21(3), 511–18.
Schäfer, A., Tauch, A., Jäger, W., Kalinowski, J., Thierbach, G. & Pühler, A. (1994) Small mobilizable multi-purpose cloning vectors derived from the *Escherichia coli* plasmids pK18 and pK19: selection of defined deletions in the chromosome of *Corynebacterium glutamicum*. *Gene*, 145(1), 69–73.
Scharf, B. & Schmitt, R. (2002) Sensory transduction to the flagellar motor of *Sinorhizobium meliloti*. *Journal of Molecular Microbiology and Biotechnology*, 4(3), 183–6.
Schmitt, R.d. (2002) Sinorhizobial chemotaxis: a departure from the enterobacterial paradigm. *Microbiology*, 148(3), 627–31.
Sherris, D. & Parkinson, J.S. (1981) Posttranslational processing of methyl-accepting chemotaxis proteins in *Escherichia coli*. *Proceedings of the National Academy of Sciences*, 78(10), 6051–5.
Shrestha, M., Compton, K.K., Mancl, J.M., Webb, B.A., Brown, A.M., Scharf, B.E. et al. (2018) Structure of the sensory domain of McpX from *Sinorhizobium meliloti*, the first known bacterial chemotactic sensor for quaternary ammonium compounds. *Biochemical Journal*, 475(24), 3949–62.
Simms, S.A., Stock, A.M. & Stock, J.B. (1987) Purification and characterization of the S-adenosylmethionine: glutamyl methyltransferase that modifies membrane chemoreceptor proteins in bacteria. *Journal of Biological Chemistry*, 262(18), 8537–43.
Simon, R., O'connell, M., Labes, M. & Pühler, A. (1986) Plasmid vectors for the genetic analysis and manipulation of rhizobia and other gram-negative bacteria. *Methods in Enzymology*, 118, 640–59.
Sobe, R.C., Gilbert, C., Vo, L., Alexandre, G. & Scharf, B.E. (2022) FliL and its paralog MotF have distinct roles in the stator activity of the *Sinorhizobium meliloti* flagellar motor. *Molecular Microbiology*, 118(3), 223–43.
Some, D., Amartely, H., Tsadok, A. & Lebendiker, M. (2019) Characterization of proteins by size-exclusion chromatography coupled to multi-angle light scattering (SEC-MALS). *Journal of Visualized Experiments*, 148, e59615.
Sourjik, V. & Schmitt, R. (1996) Different roles of CheY1 and CheY2 in the chemotaxis of *Rhizobium meliloti*. *Molecular Microbiology*, 22(3), 427–36.
Sourjik, V. & Schmitt, R. (1998) Phosphotransfer between CheA, CheY1, and CheY2 in the chemotaxis signal transduction chain of *Rhizobium meliloti*. *Biochemistry*, 37(8), 2327–35.
Sourjik, V., Sterr, W., Platzer, J., Bos, I., Haslbeck, M. & Schmitt, R. (1998) Mapping of 41 chemotaxis, flagellar and motility genes to a single region of the *Sinorhizobium meliloti* chromosome. *Gene*, 223(1–2), 283–90.
Sourjik, V. & Wingreen, N.S. (2012) Responding to chemical gradients: bacterial chemotaxis. *Current Opinion in Cell Biology*, 24(2), 262–8.
Spiro, P.A., Parkinson, J.S. & Othmer, H.G. (1997) A model of excitation and adaptation in bacterial chemotaxis. *Proceedings of the National Academy of Sciences*, 94(14), 7263–8.
Stock, J., Ninfa, A. & Stock, A. (1989) Protein phosphorylation and regulation of adaptive responses in bacteria. *Microbiological Reviews*, 53(4), 450–90.
Szurmant, H., Muff, T.J. & Ordal, G.W. (2004) Bacillus subtilis CheC and FliY are members of a novel class of CheY-P-hydrolyzing proteins in the chemotactic signal transduction cascade. *Journal of Biological Chemistry*, 279(21), 21787–1792.
Tu, Y. (2013) Quantitative modeling of bacterial chemotaxis: signal amplification and accurate adaptation. *Annual Review of Biophysics*, 42, 337–59.
Varadi, M. & Velankar, S. (2022) The impact of AlphaFold protein structure database on the fields of life sciences. *Proteomics*, 23, 2200128.
Vladimirov, N. and V. Sourjik. (2009) Chemotaxis: how bacteria use memory. *Biological chemistry*, 390(11), 1097–1104.
Wadhams, G.H. & Armitage, J.P. (2004) Making sense of it all: bacterial chemotaxis. *Nature Reviews Molecular Cell Biology*, 5(12), 1024–37.
Walukiewicz, H.E., Tohidifar, P., Ordal, G.W. & Rao, C.V. (2014) Interactions among the three adaptation systems of *Bacillus subtilis* chemotaxis as revealed by an in vitro receptor-kinase assay. *Molecular Microbiology*, 93(6), 1104–18.
Webb, B.A., Compton, K.K., del Campo, J.S.M., Taylor, D., Sobrado, P. & Scharf, B.E. (2017) *Sinorhizobium meliloti* chemotaxis to multiple amino acids is mediated by the chemoreceptor McpU. *Molecular Plant-Microbe Interactions*, 30(10), 770–7.
Webb, B.A., Hildreth, S., Helm, R.F. & Scharf, B.E. (2014) *Sinorhizobium meliloti* chemoreceptor McpU mediates chemotaxis toward host plant exudates through direct proline sensing. *Applied and Environmental Microbiology*, 80(11), 3404–15.
Webb, B.A., Karl Compton, K., Castañeda Saldaña, R., Arapov, T.D., Keith Ray, W., Helm, R.F. et al. (2017) *Sinorhizobium meliloti* chemotaxis to quaternary ammonium compounds is mediated by the chemoreceptor McpX. *Molecular Microbiology*, 103(2), 333–46.
Weis, R.M. & Koshland, D.E., Jr. (1988) Reversible receptor methylation is essential for normal chemotaxis of *Escherichia coli* in gradients of aspartic acid. *Proceedings of the National Academy of Sciences*, 85(1), 83–87.
Welch, M., Oosawa, K., Aizawa, S. & Eisenbach, M. (1993) Phosphorylation-dependent binding of a signal molecule to the flagellar switch of bacteria. *Proceedings of the National Academy of Sciences*, 90(19), 8787–91.
Wu, J., Li, J., Li, G., Long, D.G. & Weis, R.M. (1996) The receptor binding site for the methyltransferase of bacterial chemotaxis is distinct from the sites of methylation. *Biochemistry*, 35(15), 4984–93.
Yan, X.-F., Xin, L., Yen, J.T., Zeng, Y., Jin, S., Cheang, Q.W. et al. (2018) Structural analyses unravel the molecular mechanism of cyclic di-GMP regulation of bacterial chemotaxis via a PilZ adaptor protein. *Journal of Biological Chemistry*, 293(1), 100–111.
Yang, W. & Briegel, A. (2020) Diversity of bacterial chemosensory arrays. *Trends in Microbiology*, 28(1), 68–80.
Yonekawa, H., Hayashi, H. & Parkinson, J. (1983) Requirement of the cheB function for sensory adaptation in *Escherichia coli*. *Journal of Bacteriology*, 156(3), 1228–35.
Zatakia, H.M., Arapov, T.D., Meier, V.M. & Scharf, B.E. (2018) Cellular stoichiometry of methyl-accepting chemotaxis proteins in *Sinorhizobium meliloti*. *Journal of Bacteriology*, 200(6), e00614-17.
Zhao, R., Collins, E.J., Bourret, R.B. & Silversmith, R.E. (2002) Structure and catalytic mechanism of the *E. coli* chemotaxis phosphatase CheZ. *Nature Structural Biology*, 9(8), 570–5.

SUPPORTING INFORMATION

Additional supporting information can be found online in the Supporting Information section at the end of this article.

How to cite this article: Agbekudzi, Alfred, Timofey D. Arapov, Ann M. Stock and Birgit E. Scharf 2024. "The dual role of a novel *Sinorhizobium meliloti* chemotaxis protein CheT in signal termination and adaptation." *Molecular Microbiology* 122: 429–446. https://doi.org/10.1111/mmi.15303.

Supplemental Fig S1

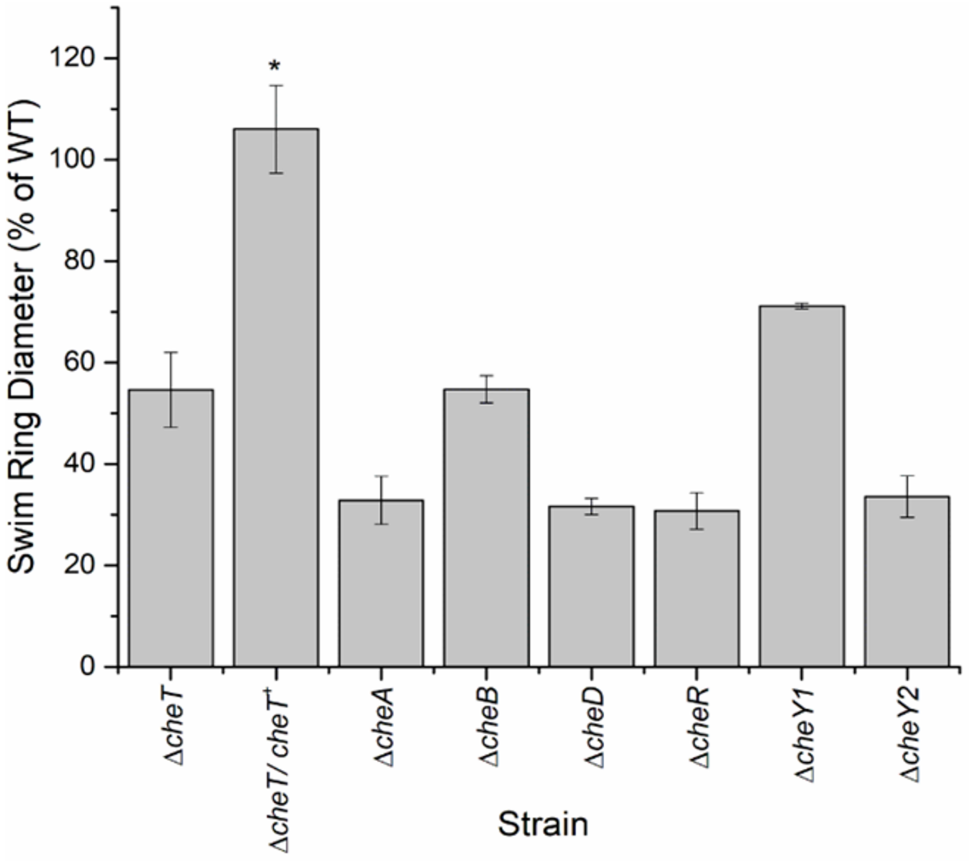

Supplemental Fig S2

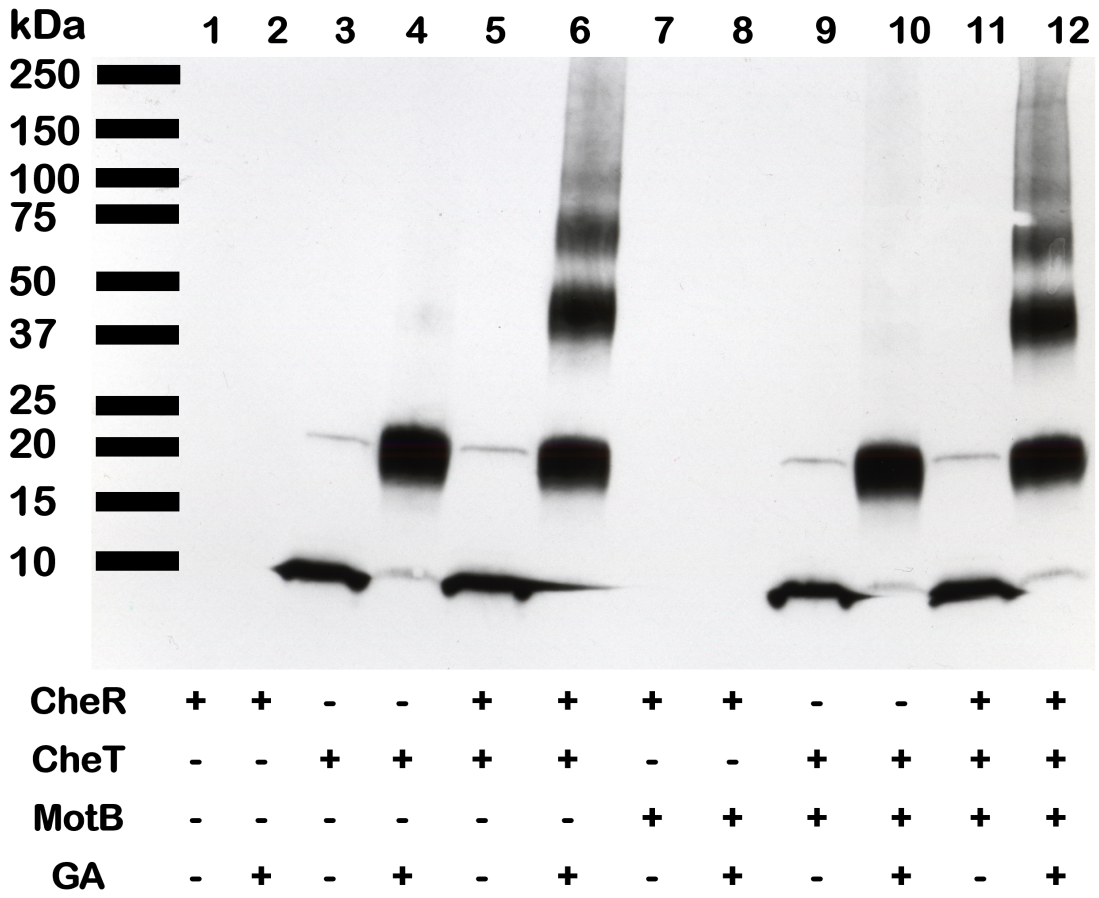

Supplemental Fig S3